Structural setting and geodynamics of the Kvarner area (Northern Adriatic)

Marko Špelić [a], Anna Del Ben [b,*], Krešimir Petrinjak [a]

[a] *Croatian Geological Survey, Department of Geology, Sachsova 2, Zagreb, 10000, Croatia*
[b] *University of Trieste, Department of Mathematics and Geosciences, Via Weiss 1, 34128, Trieste, Italy*

A B S T R A C T

The Kvarner area is located in the Northern Adriatic Sea, between the south-east Istrian Swell, the Rijeka coast and the Croatian sea boundary. It includes several islands, representing the outcropping parts of anticlines produced by the compressional/transpressional deformation of the External Dinaric Chain. An extensive 2D seismic dataset, acquired for hydrocarbon exploration and calibrated by wells, allowed us to reconstruct the time structural maps in Kvarner and unravel its regional fault pattern. The Dinaric compressional phase affected the area in the Late Cretaceous, with both thin- and thick-skinned tectonics related to Adriatic Carbonate Platform (AdCP) succession rigidity. Structural highs facing the Kvarner offshore from the Istrian inland continue through the Kvarner and Rijeka bays and outcrop in the islands. These anticlines, originating from the pre-Messinian Dinaric thrust system, were reactivated by the post-Messinian transpression, as testified by flower structures. Several sharp valleys represent two main low structural lineaments, developed between the anticlines and partially incised during the Messinian. They were observed throughout the entire studied area, specifically in the western part of the bays, where the lineament continues through the valleys and penetrates the SW-Istria land. Data show that the Messinian erosional effect and sedimentation patterns were influenced and driven by the morphology of older structures produced by the Dinaric compressional phase.

1. Introduction

As part of the Adria Plate, situated between external Dinarides and Istria foreland (Schmid et al., 2020), the Kvarner area has been affected by complex tectonic interactions (Korbar, 2009; Placer et al., 2010; van Hinsbergen et al., 2020). The external Dinaric deformation on the Kvarner area created an alternation of structural highs and lows between the Istrian Plateau, the northern Kvarner Islands and the Dugi Otok Plain. Previous geological research of the study area was generally based on the analysis of the structures and stratigraphic sequences outcropping in the coastal regions (GKSFRJ, 1970; Vlahović et al., 2005; GKRH, 2009; Korbar, 2009 and references therein; Brčić et al., 2017) or offshore datasets (e.g., Prelogović, 1995; Grandić et al., 1999, 2002; Del Ben, 2002; Finetti and Del Ben, 2005; Busetti et al., 2010a, b; Cazzini et al., 2015; Velić et al., 2015), making a correlation between the Istrian and the northern Dalmatian Islands geology (e.g., Vlahović et al., 2005; Korbar, 2009). The thick carbonates that characterizes the study area represent a very compact lithology, which involves a high resistance to deformation and consequent reduced plastic deformation. Furthermore, the seismic facies of the carbonate platform are generally opaque, and

the classical criteria useful for interpreting fault systems, such as reflectors cut-off, presence of kink bands, and evidence of fault planes (Shaw et al., 2004), are difficult to recognize. All of this represents a major problem that can be solved using many data covering the whole area. In this study, we used all evidence emerging from a large number of newly available seismic profiles to enhance the most significant discontinuities that accommodate the deformations. To do this, we analyzed and described different seismic facies and related them to the main deformational events. The obtained time structural maps were compared with surface geological maps to examine the main structures and relationships between recent and ancient morphology. Therefore, this study attempts to describe the relationship between observed structures, lineaments and different tectonic phases of the Kvarner region, situated in the complex contact zone between the external Dinarides (Dalmatian and High Karst units, Schmid et al., 2020), the foreland area of the Istrian Peninsula and the Adriatic foreland.

2. Geological setting

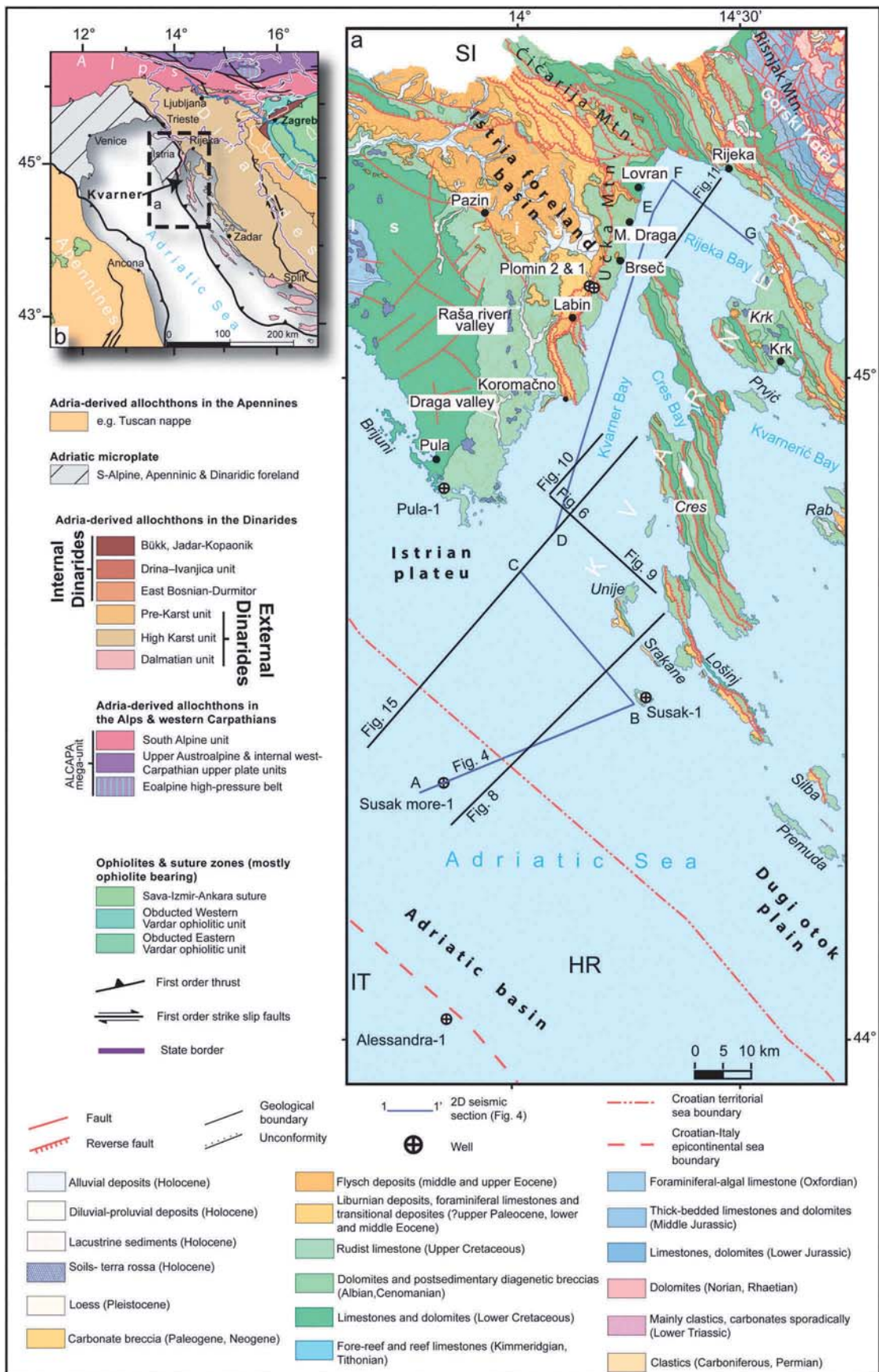The Kvarner area is located in the contact between the Adriatic basin,

---

Fig. 1. Local geological (a) and regional geotectonic setting (b) of the study area (after Schmid et al., 2020; GKRH, 2009; https://www.azu.hr/en).
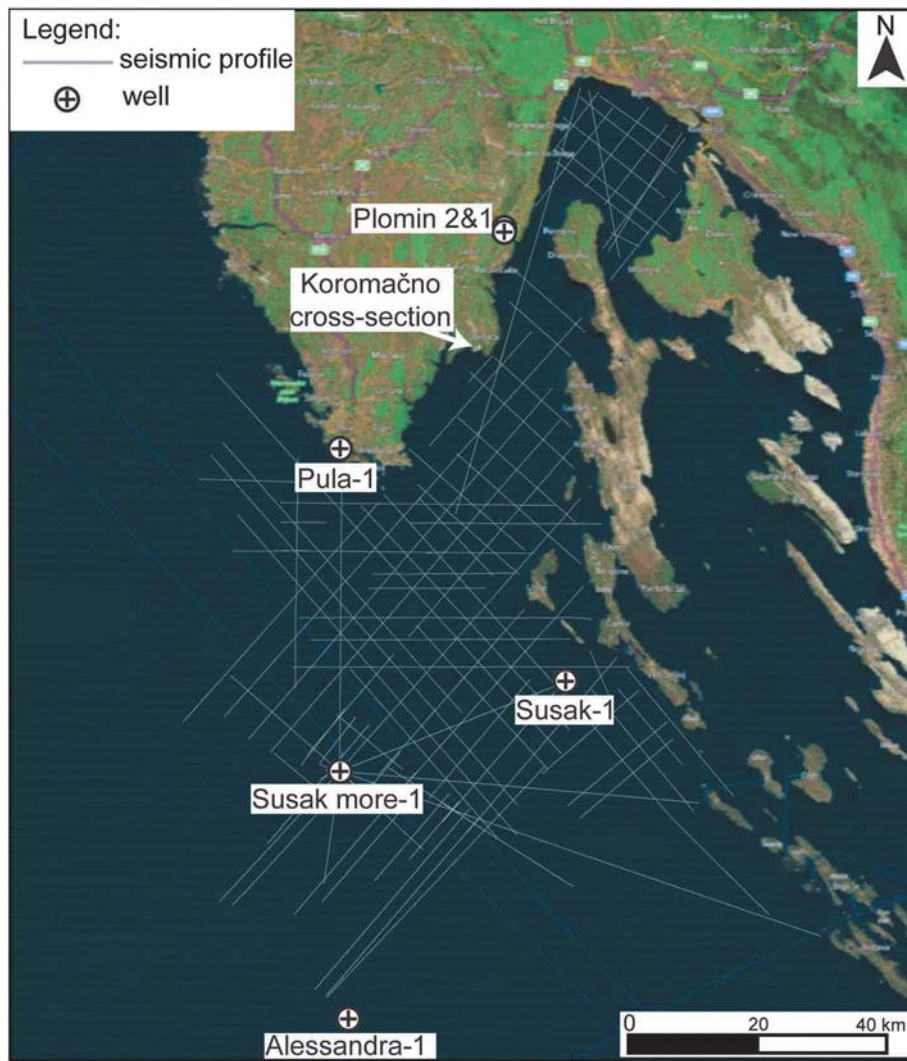
Legend (a, b):

Adria-derived allochthons in the Apennines
- e.g. Tuscan nappe

Adriatic microplate
- S-Alpine, Apenninic & Dinaridic foreland

Adria-derived allochthons in the Dinarides

Internal Dinarides
- Bükk, Jadar-Kopaonik
- Drina–Ivanjica unit
- East Bosnian-Durmitor

External Dinarides
- Pre-Karst unit
- High Karst unit
- Dalmatian unit

Adria-derived allochthons in the Alps & western Carpathians (ALCAPA mega-unit)
- South Alpine unit
- Upper Austroalpine & internal west-Carpathian upper plate units
- Eoalpine high-pressure belt

Ophiolites & suture zones (mostly ophiolite bearing)
- Sava-Izmir-Ankara suture
- Obducted Western Vardar ophiolitic unit
- Obducted Eastern Vardar ophiolitic unit

— First order thrust
— First order strike slip faults
— State border

Fault
Reverse fault
Geological boundary
Unconformity
1———1' 2D seismic section (Fig. 4)
⊕ Well
—·—·— Croatian territorial sea boundary
——— Croatian-Italy epicontinental sea boundary

- Alluvial deposits (Holocene)
- Diluvial-proluvial deposits (Holocene)
- Lacustrine sediments (Holocene)
- Soils- terra rossa (Holocene)
- Loess (Pleistocene)
- Carbonate breccia (Paleogene, Neogene)
- Flysch deposits (middle and upper Eocene)
- Liburnian deposits, foraminiferal limestones and transitional deposites (?upper Paleocene, lower and middle Eocene)
- Rudist limestone (Upper Cretaceous)
- Dolomites and postsedimentary diagenetic breccias (Albian, Cenomanian)
- Limestones and dolomites (Lower Cretaceous)
- Fore-reef and reef limestones (Kimmeridgian, Tithonian)
- Foraminiferal-algal limestone (Oxfordian)
- Thick-bedded limestones and dolomites (Middle Jurassic)
- Limestones, dolomites (Lower Jurassic)
- Dolomites (Norian, Rhaetian)
- Mainly clastics, carbonates sporadically (Lower Triassic)
- Clastics (Carboniferous, Permian)

Map labels (a): SI, Čičarija Mtn., Istria foreland basin, Rijeka, Lovran, F, E, M. Draga, G, Plomin 2 & 1, Brseč, Rijeka Bay, Pazin, Labin, Raša river valley, Risnjak Mtn., Gorski Kotar, Krk, Prvić, Koromačno, Draga valley, Brijuni, Pula, Pula-1, Istrian plateu, Cres Bay, Cres, Rab, D, C, Unije, Kvarner Bay, Fig. 10, Fig. 6, Fig. 9, Srakane, Lošinj, Susak-1, B, Silba, Fig. 15, Fig. 4, A, Susak more-1, Fig. 8, Adriatic Sea, Premuda, Dugi otok plain, Adriatic basin, HR, IT, Adriatic basin, Alessandra-1, 0 5 10 km

Map labels (b): Alps, Ljubljana, Trieste, Venice, Istria, Rijeka, Zagreb, Kvarner, a, Adriatic Sea, Ancona, Zadar, Split, Apennines, Dinarides, 0 100 200 km

Fig. 2. Position map of the available dataset composed of seismic profiles and wells (https://www.google.com/intl/hr/earth/).

the Dinarides orogen system and the Istrian Swell (Fig. 1). It is part of the lithospheric plate named Adria or Adriatic microplate (van Hinsbergen et al., 2020). Several orogenic systems formed as a consequence of Adria convergence with European plate lithosphere units including the Dinarides orogen (Schmid et al., 2020 and references therein).

The separation of Adria from the African plate by continental rifting processes began in the Middle Triassic (Channell et al., 1979), while newer findings suggest the Permian age (e.g., Stampfli, 2005). The extension was associated to crustal-scale normal faults and the creation of horst and half-graben structures (Tari, 2002; Grandić et al., 2002; Finetti and Del Ben, 2005). The passive continental margin in the South Tethys realm also comprised the paleogeographical area of a large South Tethyan carbonate platform, after which, in the Lower Jurassic (Toarcian), the distinct Adriatic (AdCP, Vlahović et al., 2005) and Apulia (ApCP, Zappaterra, 1990; Mattavelli et al., 1991; Nicolai and Gambini, 2007) carbonate platforms developed. The AdCP slope also formed in Toarcian (Grandić et al., 2010) as a transitional area to the newly formed Adriatic basin (Vlahović et al., 2005). The beginning of convergence between Adria and Tisza-Dacia (part of the Eurasian lithosphere plate) is marked by the Middle Jurassic intra-oceanic subduction (Pamić et al., 1998; Tari, 2002; van Hinsbergen et al., 2020). Continuous convergence processes formed prominent structural features, such as the Lower Cretaceous Istrian anticline (Polšak and Šikić, 1973; Matičec et al., 1996).

During the Late Cretaceous, continental collision processes took place (Bennet et al., 2008; Müller et al., 2019). In external Dinarides, this process is denoted by the influence of synsedimentary compressional deformation (Prtoljan et al., 2007; Brčić et al., 2017) and the cessation of AdCP deposition due to regional emersion (Vlahović et al., 2005; Korbar, 2009). Syn-orogenic deformation in external Dinarides caused in-sequence, thin- and thick-skinned thrusting (Prelogović, 1995; Del Ben, 2002; Tari, 2002; Vlahović et al., 2005; Tomljenović et al., 2009; Korbar, 2009; van Unen et al., 2019) and the development of the Paleogene foreland basin (Babić et al., 2008). Tectonic shortening created structures with SW vergence (Fig. 1a), such as fault-bend folds (Tari, 2002) and thrust-nappe structures (Busetti et al., 2010b; Palenik et al., 2019).

Neogene to Quaternary geodynamic processes of the Adria were controlled by CCW rotation and fragmentation (Placer et al., 2010; le Breton et al., 2017). Furthermore, the evolution of the neighboring Pannonian basin system (Žibret and Vrabec, 2016; Bada et al., 2007), orogenesis in the Apennines (Bigi et al., 1992; Del Ben and Oggioni, 2016; Brancolini et al., 2019), gravity gliding and dextral wrenching in the Dinarides and in their contact zone with the Istrian tectonic block (Korbar, 2009; Placer et al., 2010; Tomljenović et al., 2013; Palenik et al., 2019) played a crucial role in the structural evolution of the Kvarner area. In the external Dinarides, the stress field orientation changed several times during Neogene, from NE–SW extension and E–W compression to N–S extension (Žibret and Vrabec, 2016). Consequently, older structures were reactivated as strike-slip structures of NE–SW and
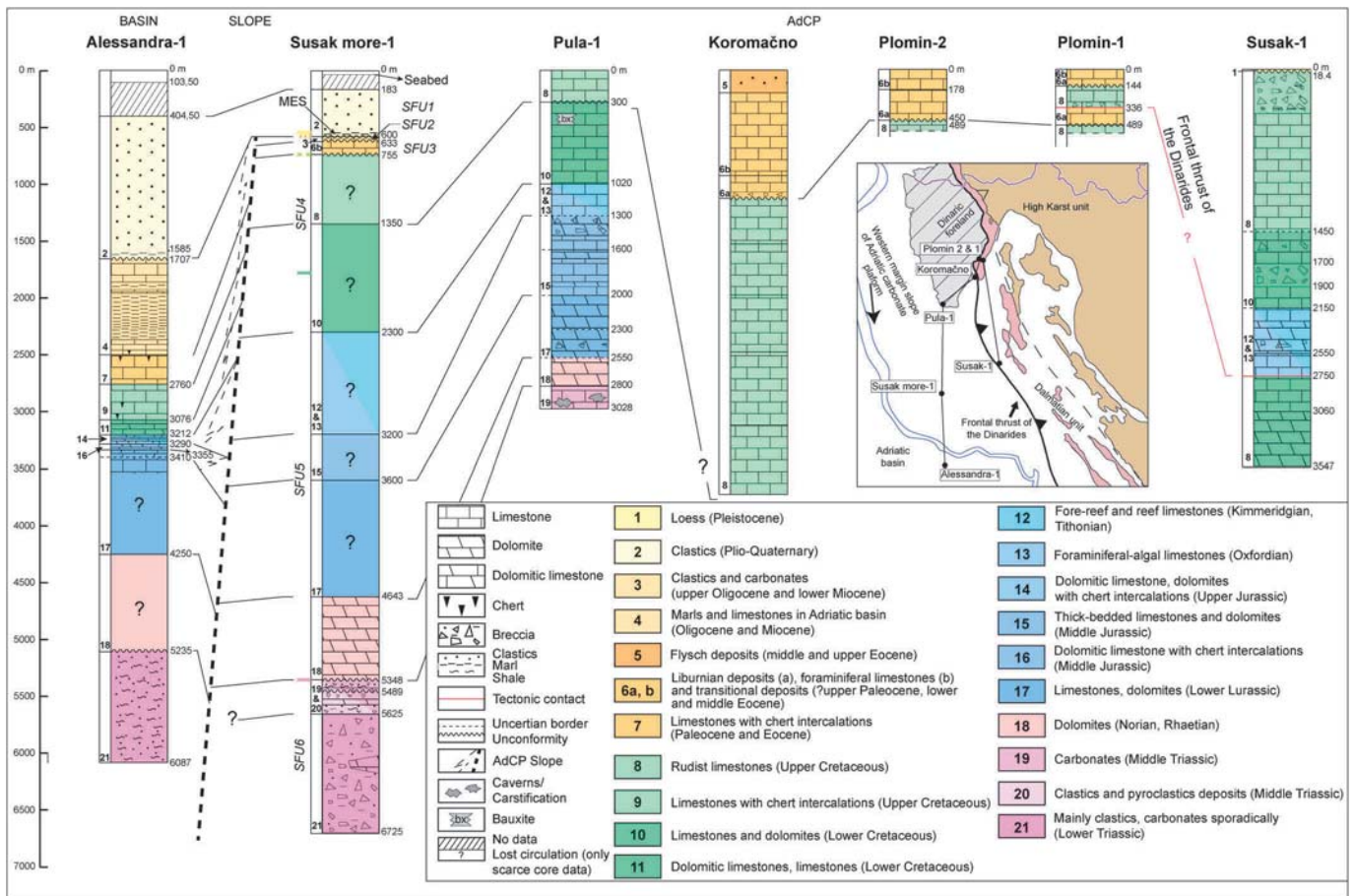
3

Fig. 3. Position (inset) and stratigraphic correlation of wells available in the study area (after Magaš, 1965; Grandić et al., 1999, Grandić et al., 2013; Velić et al., 2015; Schmid et al., 2020).

NW–SE orientation, caused by recent N–S compression and E–W tension (Palenik et al., 2019). Otherwise, Ustaszewski et al. (2014) state NE–SW compression. These structures are the primary seismogenic sources during the Quaternary in the Kvarner area or, more precisely, in the city of Rijeka and its surrounding region (Del Ben et al., 1991; Tomljenović et al., 2009; Kastelic and Carafa, 2012; Palenik et al., 2019).

As noted, structural evolution played an essential role in sedimentation and vice versa (e.g., influence of depth of Jurassic to Early Cretaceous decollement on the width and size of the belt, in agreement with Tari, 2002). Carboniferous-Permian clastites, Lower Triassic mixed siliciclastic-carbonate, and regionally present Upper Triassic carbonates (*main dolomite or Hauptdolomit/Dolomia Principale*, Velić et al., 2003) are referred to as the AdCP basement by Vlahović et al. (2005). Outcrops can be found in the neighboring Gorski Kotar region (Fig. 1a), and deep wells also penetrated them in the Kvarner and Istria region (Fig. 4, Grandić et al., 1999). The oldest unit of AdCP outcropping in Kvarner comprises Lower Cretaceous carbonates (Fig. 1a). Those from the Lower and Upper Jurassic are present in the subsurface and were recovered by wells (e.g., Susak-1; Fig. 3). The combined thickness of AdCP deposits can reach 5000 m (Vlahović et al., 2005) and they generally consist of shallow-water and rarely deeper-water carbonates (Vlahović et al., 2005; Brčić et al., 2017), as well as several stratigraphic levels of emersion and associated bauxites (Velić et al., 2003).

Only locally present, lower Paleocene brackish to freshwater Kozina limestones (Korbar, 2009) transgressively overlie karstified Mesozoic carbonates (Velić et al., 2003). Eocene foraminiferal limestones of the marine carbonate ramp mark the deepening of the new foreland basin (Ćosović et al., 2004). Cenozoic carbonate breccia (Vlahović et al., 2018) covers parts of Krk Island and a small area, situated 10 km to the

SE from the city of Rijeka (Fig. 1), marking the zones of regional structures, such as thrust and hinges of anticlines (Šušnjar et al., 1970). Middle Eocene turbidite flysch deposits (Babić et al., 2008) consist of marl and sandstones alternation (Bergant et al., 2003; Marjanac and Marjanac, 2007), with occasional occurrence of megaturbidites or "megabed" (Marjanac, 1996; Placer et al., 2004). The thickness of flysch deposits is usually reduced or increased by erosion and structural deformation (Velić et al., 2015), specifically by incorporating thrust-nappe structures such as Učka Mt. (Fig. 1).

In the Kvarner area, there are no outcrops of Neogene age (Fig. 1). However, Miocene limestones (Fig. 3) and marine clastites are common offshore (Grandić et al., 1999; Vaniček, 2013; Velić et al., 2015) and nearby coastal areas (Pag Isle, Jiménez-Moreno et al., 2009). The subsequent Messinian salinity crisis (Capella et al., 2019) caused significant erosion and accompanying deposition of siliciclastic sediments and evaporites (Lofi, 2018; Vaniček, 2013, Velić et al., 2015). Unconsolidated Pliocene sediments are typical in offshore areas, consisting of alternating clays and sands (Velić and Malvić, 2011; Brancolini et al., 2019), while no onshore outcrops are found in the Kvarner area (Fig. 1a). In contrast, Quaternary sediments are typical on the surface of the Kvarner (Fig. 1a), with the exceptional thickness of Late Pleistocene sediments up to 90 m occurring in the Susak Island (Wacha et al., 2011). Moreover, Late Pleistocene and Holocene sediments have been proven in submerged areas between islands, such as the Rijeka Bay or Lošinj Channel (Juračić et al., 1999; Brunović et al., 2020).

3. Methods and data

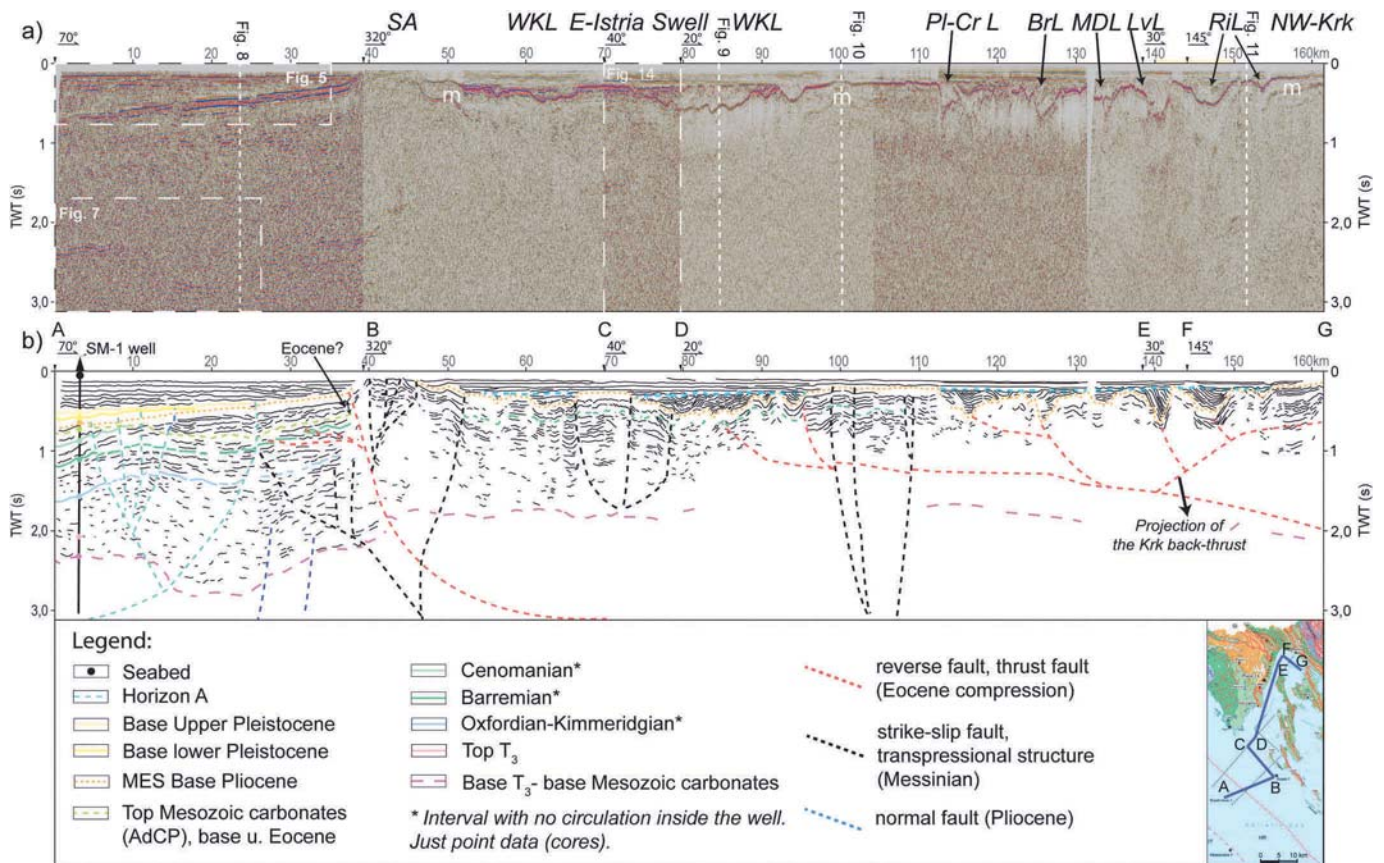Surface and subsurface data were analyzed and interpreted.

Fig. 4. Regional composite seismic section from the Adriatic Sea axis to the Rijeka coast, crossing the entire Kvarner area, between the SE-Istrian coast and the Lošinj/Cres/Krk Islands. (a) Uninterpreted profile and (b) line-drawing. Boxes in (a) are the details represented in the following pointed figures. **SA:** Susak Anticline, **WKL:** West Kvarner lineament, **Pl-Cr L:** Plomin-Cres Bay lineament, **BrL:** Brseč low, **MDL:** Mošćenička Draga low, **LvL:** Lovran low, **RiL:** Rijeka low, **SM:** Susak more-1, **m:** multiples.

Structural and stratigraphic measurements were gathered during the GEOSEKVA project or from vintage chronostratigraphic and newer lithostratigraphic maps (GKRH, 2009; Fuček et al., 2012; Fuček et al., 2015), using standardized geological mapping techniques.

Subsurface data consist of 2D seismic reflection sections and well data. Seismic sections were recorded during the hydrocarbon exploration of the INA d.d. company, which was used with the permission of CHA (https://www.azu.hr/en). The positive polarity of the seismic data is represented in red. Other original recording and processing parameters are unknown. We analyzed more than 200 sections covering 2307 km² in the Croatian offshore (Fig. 2), recorded up to 6 s two-way traveltime (TWT). The sections were compared with Italian CROP project data, which are available through the ViDEPI project (https://www.videpi.com/videpi/videpi.asp).

Well data were also obtained during hydrocarbon exploration from 1960 to the 1980s. Original stratigraphic and technical reports were digitized and systemized. The seismic-well calibration was performed by constructing synthetic seismograms. This critical step allowed for the anchoring of lithological units to corresponding seismic facies (Fig. 3). Information on interval velocity has been used to transform the well data into the TWT thickness of the time-migrated seismic data and to estimate the depths and thicknesses of units in meters along the interpreted profiles.

Seismic characteristics of different lithological units were classified after regional interpretation of the available seismic data, regardless of the limitations imposed by the vertical seismic resolution. The "Rayleigh's Limit of Vertical Resolution" states that two events must be separated by a distance of at least ¼ of the wavelength to be individually recognizable, thus not allowing for the identification of thinner units. By

a calculation of the number of waves in the upper depth of 1 s, the distance can be assumed to be at least 10–15 m and 15–20 m, respectively, in the upper and lower Plio-Quaternary sequences. For the time structural map construction, the convergent interpolation and normal extrapolation method, with a grid of 50 × 50 m were used in the Schlumberger Petrel 2019.2 software. Surfaces were smoothed in up to 10 iterations with filter width value 1.

4. Seismic facies description

The seismic profiles interpreted in this study highlight the presence of several main seismic facies units (SFUs). The mapped deposits in the research area are in a stratigraphic range from the Lower Triassic to Quaternary (Fig. 4 and Table 1).
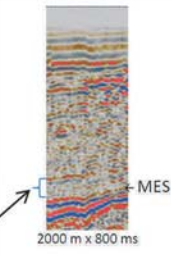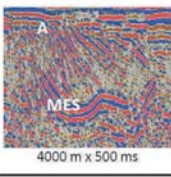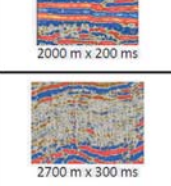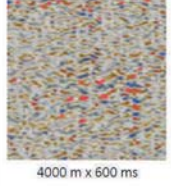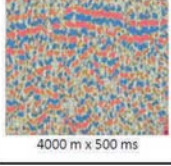
Susak more-1 penetrated the entire AdCP deposits and reached the Triassic clastic sequence, calibrating all main seismic facies in the study area (Fig. 3). Susak more-1 calibrates the profile representing the first SW–NE part of the composite profile shown in Fig. 4. Susak-1 is located on the Susak island, calibrating the uplifted lithological Cretaceous sequences. Other wells are present in or close to the study area (Fig. 2), furnishing important information about the region's stratigraphy and changeable thicknesses of the AdCP and Eocene Flysch deposits. The different stratigraphic units (seismic facies unit) are numbered from top to bottom (Fig. 3).

The seismic stratigraphic framework was defined as a reference (Table 1). It also allowed for the recognition of units away from wells.

The most recognizable reflectors are typical: i) the base of the Plio-Quaternary (PQ) or top of the pre-Pliocene sequence, also known as the Messinian erosional surface (MES), ii) the top of the carbonates, and

Table 1
Geological information and related seismic stratigraphy of the interpreted seismic facies units (SFUs).

| Lithological unit	Depositional environment	Age	Reflection geometry	Amplitude	Seismic facies unit (SFU)	Seismic facies example
Sand, silt and clay	Shallow marine/inner shelf, heterogeneous	Upper Pleistocene	Often muted in the upper part, parallel, continuous above, discontinuous below	Medium to high amplitude	SFU1	2000 m x 800 ms
Sand, silt and clay	Shallow marine/inner shelf, heterogeneous	Lower Pleistocene	Wedge-shaped reflectors, only in the western part of the study area	Medium to low amplitude		
Clay	Marine	Upper Pliocene	Thin, irregular thickness. Gradually east-ward thinning	Low amplitude, based on high amplitude MES	SFU2	
Sand/shale successions and fine grained deposits	Shallow marine to lacustrine, rapid filling of valleys	Messinian (?) to Pliocene	Generally, clinoform geometry; baselapping the MES and offlapping the unconformity "A"	Medium amplitude	SFU2-3	4000 m x 500 ms
Carbonate, fossiliferous limestone	Shallow marine	Late Oligocene to early Miocene	Thin reflectors, indistinct in a seismic package topped by MES	High amplitude	SFU3	2000 m x 200 ms
Breccia, Flysch	Alluvial fans, rockfall breccias, tectonic breccias, deep marine (foredeep)	Eocene to Early Oligocene	Low amplitude, discontinuous stratification	Medium to low amplitude	SFU3	2700 m x 300 ms
Transitional deposits	Deeper marine	Middle Eocene	Below seismic resolution			
Foraminiferal limestones	Sub-littoral, forebank, peri-reef, open-marine; generally, from shallow to deep marine	Early to Middle Eocene	Parallel discontinuous	Low amplitude, low frequency	SFU3	3000 m x 200 ms
Kozina beds	Freshwater to brackish	Paleocene	Below seismic resolution			
Upper portion of carbonates	Shallow marine	Cretaceous	Locally continuous, parallel and tilted reflectors with erosional truncations	Medium to high	SFU4	4000 m x 600 ms
Middle to lower portion of carbonates	Shallow marine	Late Triassic to Jurassic	Transparent, semi-transparent, locally fractures and tilted reflectors	Low amplitude, low frequency, semi-opaque	SFU5	4000 m x 600 ms
Clastic sequence	Continental environment	Lower to Middle Triassic	Continuous at the top, discontinuous bellow	High amplitude, low frequency at the top	SFU6	4000 m x 500 ms
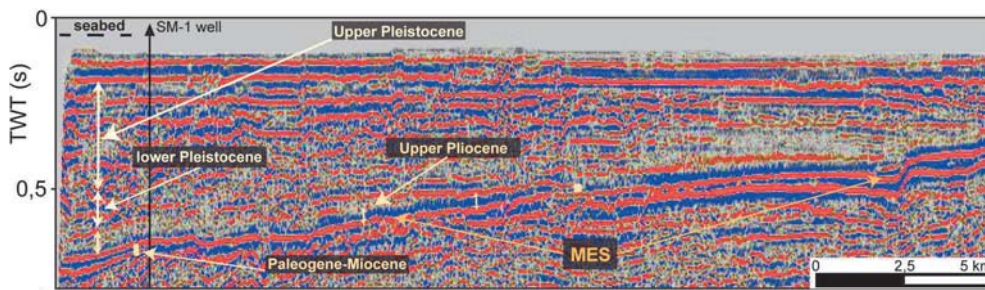
Fig. 5. Detail of the composite profile of Fig. 4: calibration by Susak more-1 well evidences the high amplitude Cenozoic packages; their thicknesses are at the limit of vertical seismic resolution. Note toplap termination of the Miocene-Paleogene layers on the left part of the profile. Vertical exaggeration is x10. See position in Fig. 2.
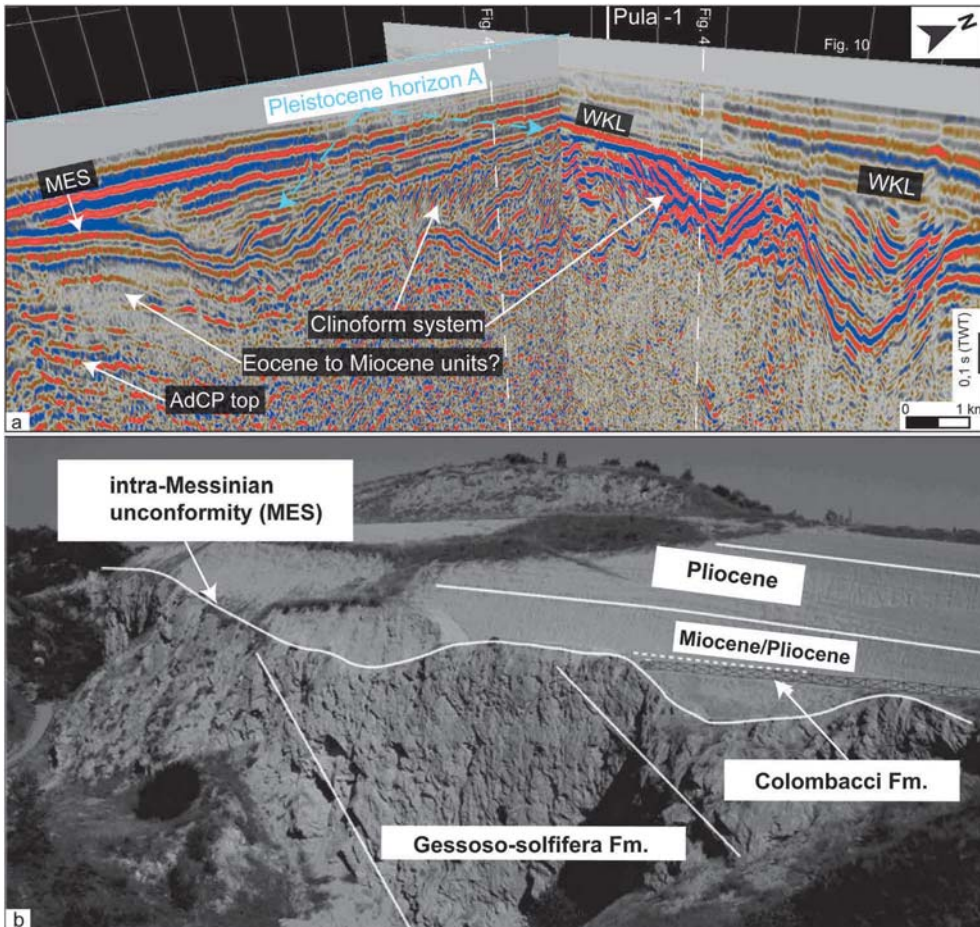

Fig. 6. (a) Parts of two crossing orthogonal seismic sections on the Istrian Swell: the clinoform systems fill the channels with base-lap termination on the MES unconformity. In the lower part of the profile, the upper portion of the AdCP is evidenced by semi-transparent seismic facies; the age of the filling sequence, never calibrated by wells, is hypothesized to be Plio-Quaternary. A plausible Late Messinian alternative age is suggested by a comparison with (b) the Colombacci Formation, onlapping the MES in the Northern Apennines (Italy) and topped by major Miocene/Pliocene boundary (modified by Roveri et al., 2006).

iii) the base of the carbonates or top of the Permo-Triassic clastic sequence. Other reflectors can possibly be interpreted, but their continuity throughout the study area is more difficult to follow. The base of the Plio-Quaternary and the top of the carbonates are often coincident in the study area, due to the lack or small thickness of the Paleogene/Neogene sequences. In particular, the Messinian sequence and Eocene flysch unit have not been calibrated by available wells due to their irregular presence in the Kvarner coastal area (Fig. 1). In the Lower Cretaceous sequence, the Susak more-1 well calibrates a seismic reflector that we could only interpret and map in the western part of the study area.

4.1. Pleistocene unit (SFU1)

The upper limit of the PQ sequence is the seabed (sb, Fig. 5).

Unfortunately, the shallowest part of the seismic profiles has been muted, so that often the "sb" reflector is not seen or is poorly defined (Figs. 5 and 6). In some cases, the nullifying process via muting is ambiguous. Sometimes, the first reflector is the sea bottom below the seismically transparent water layer, or in other cases, it is inner Quaternary in age. Thus, we were unable to produce an isopach map of the Plio-Quaternary sequence.

The studied area is mainly situated on a shallow northeast Adriatic Sea. The sea bed reaches a maximum depth (except the muting effect) of approximately 100 ms TWT (corresponding to 75 m if a wave velocity of 1500 m/s for the seawater is considered), near the axial line of the Adriatic Sea. The wells (Fig. 3) calibrate an indistinct Pleistocene sequence, approximately 500 m thick in the Susak more-1 well, composed of an alternation of clay, silt, and sand. Upper and lower seismic facies were recognized (Fig. 5), of the Holocene/Late Pleistocene
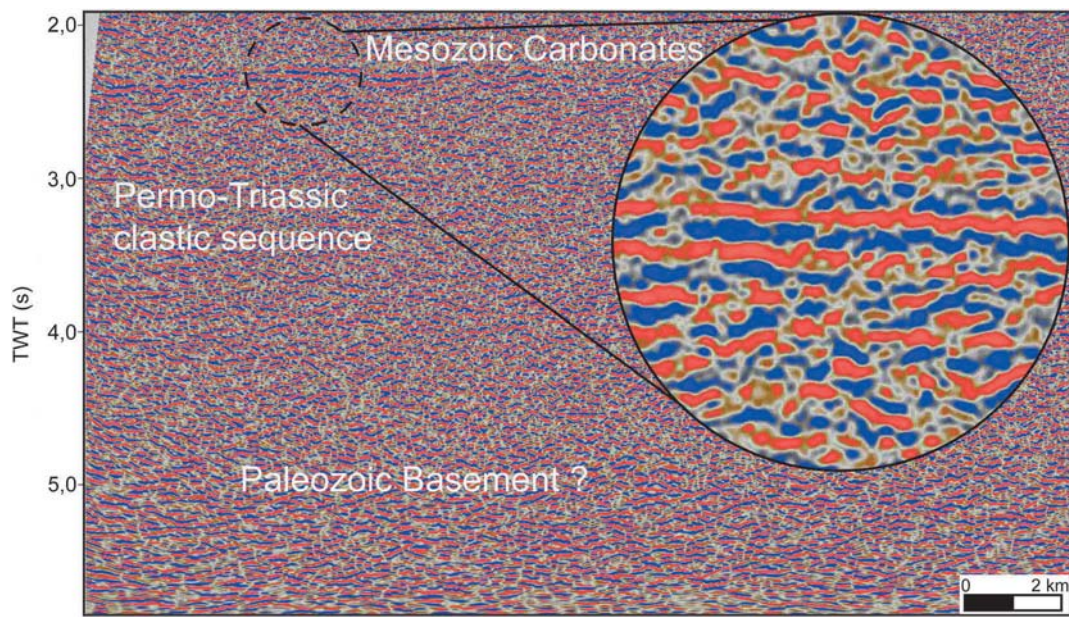
Fig. 7. Deep detail of the seismic profile sited in the western sector of the study area. High amplitude low-frequency reflectors typically characterize the seismic facies of the Permo-Triassic clastic sequence and allow to distinguish them from the upper carbonate succession.

and of the lower Pleistocene, respectively.

The Holocene/upper Pleistocene sequence is in a sub-horizontal setting. Its medium/high-amplitude reflectors are parallel and characterized by low frequencies, which may be related to a processing, focused on revealing the deeper parts of the sequence targeted by oil exploration.

The lower Pleistocene sequence exhibits eastward pinch-out and termination on a weak reflector, which is interpreted as the upper Pliocene top. The onlapping terminations suggest an increasing hiatus, until the disappearance of the lower Pleistocene toward the east (Fig. 4).

4.2. Upper Pliocene unit (SFU2)

The upper Pliocene layer is 30 m thick in the Susak more-1 well, and it is generally composed of clay rich marl and sandstone alternation. It thickens gradually toward the west and is not present or seismically resolved in the eastern part. Where it is calibrated, the layer shows semi-transparent facies with a discontinuous medium amplitude positive polarity reflector at the top, which onlaps the typically prominent reflector of the MES (Fig. 5).

The available wells do not calibrate the lower Pliocene deposits. In the Adriatic Sea, it generally has semi-transparent seismic facies, also observed in the Ionian ("PQc" sub-unit of Camerlenghi et al., 2019), Sicily Channel (Civile et al., 2014), and Tyrrhenian (Fabbri and Selli, 1972) basins, which are related to a pelagic sedimentary sequence. It was deposited after the end of the Messinian Salinity Crisis (MSC) during the Zanclean restored connection between the Atlantic Ocean and the Mediterranean Sea.

4.3. Infilling deposit above MES (SFU2-3)

Along the composite profile (Fig. 4), the MES also represents the base of prominent channels, canyons, and small basins. They are filled with discontinuous and partially deformed medium amplitude reflectors, which often exhibit clinoform geometry (Fig. 6a and Table 1), down-lapping the MES and offlapping the horizon "A". The sub-horizontal unconformity separates the clinoforms system from the Pleistocene layers and remains parallel to them. These infilling deposits directly cover the MES. If it is related to the Pliocene re-flooding, the great increase of the post-MES thickness along these features has to be totally

ascribed to the Plio-Quaternary.

A comparison with stratigraphy and geometry in the Northern Apennines (Fig. 6) suggests an alternative hypothesis. These deposits could represent a last Messinian deposition related to the Lago Mare sequence, named the Colombacci Formation, linked with fluvial-deltaic systems (Roveri et al., 2006). It is always based on an erosional truncation and covered by the Plio-Quaternary marine deposits of the Argille Azzurre formation. Typical Lago Mare Fm. is characterized by an infilling feature with Paratethyan organisms following the MSC peak and preceding the Zanclean reflooding in the Mediterranean Sea.

4.4. Eocene to Miocene units (SFU3)

The erosional character of MES is only locally recognizable (e.g. Fig. 5, left sector). In the central part, the MES seems to be approximately conformable with the underlying reflectors (Fig. 6), as observed in the SFU2-3 mentioned above. The underlying reflectors do not exhibit clear erosional truncation, which could be due to the limited seismic resolution. However, such features should not be produced only by erosion. The channels and valleys rather represent the synclines which, alternating with structural highs, were originated by deformation of the SFU3.

The Susak more-1 well calibrates 33 m of lower Miocene–upper Oligocene clastites and carbonates. Based on original reports, the underlying succession is composed of 132 m of lower Oligocene–upper Eocene fossiliferous limestone. Based on the fossil assemblage and as assumed by Grandić et al. (1999) correlation of the wells, these are Eocene foraminiferal limestones. In the Susak more-1 area, the whole Paleogene–Miocene sequence is characterized by high-amplitude reflectors, eastward converging (Fig. 5, left sector), with the top eroded by MES. It becomes very thin toward the east, where internal reflectors cannot be distinguished and the sequence exhibits chaotic seismic facies. In the onshore, maximally 700 m of Eocene carbonate ramp Foraminiferal limestone is present (Figs. 1 and 3). These deposits are divided as four sub-units, from the shallower to deeper parts of the carbonate ramp: Miliolid, Alveolinid, Numulitid, and Discocyclina limestones (Velić et al., 2003).

The flysch unit was not encountered in any of the available wells. In the Gulf of Trieste (Busetti et al., 2010a, b) and in the Isonzo Plain (Accaino et al., 2019), the Eocene terrigenous sedimentary sequence
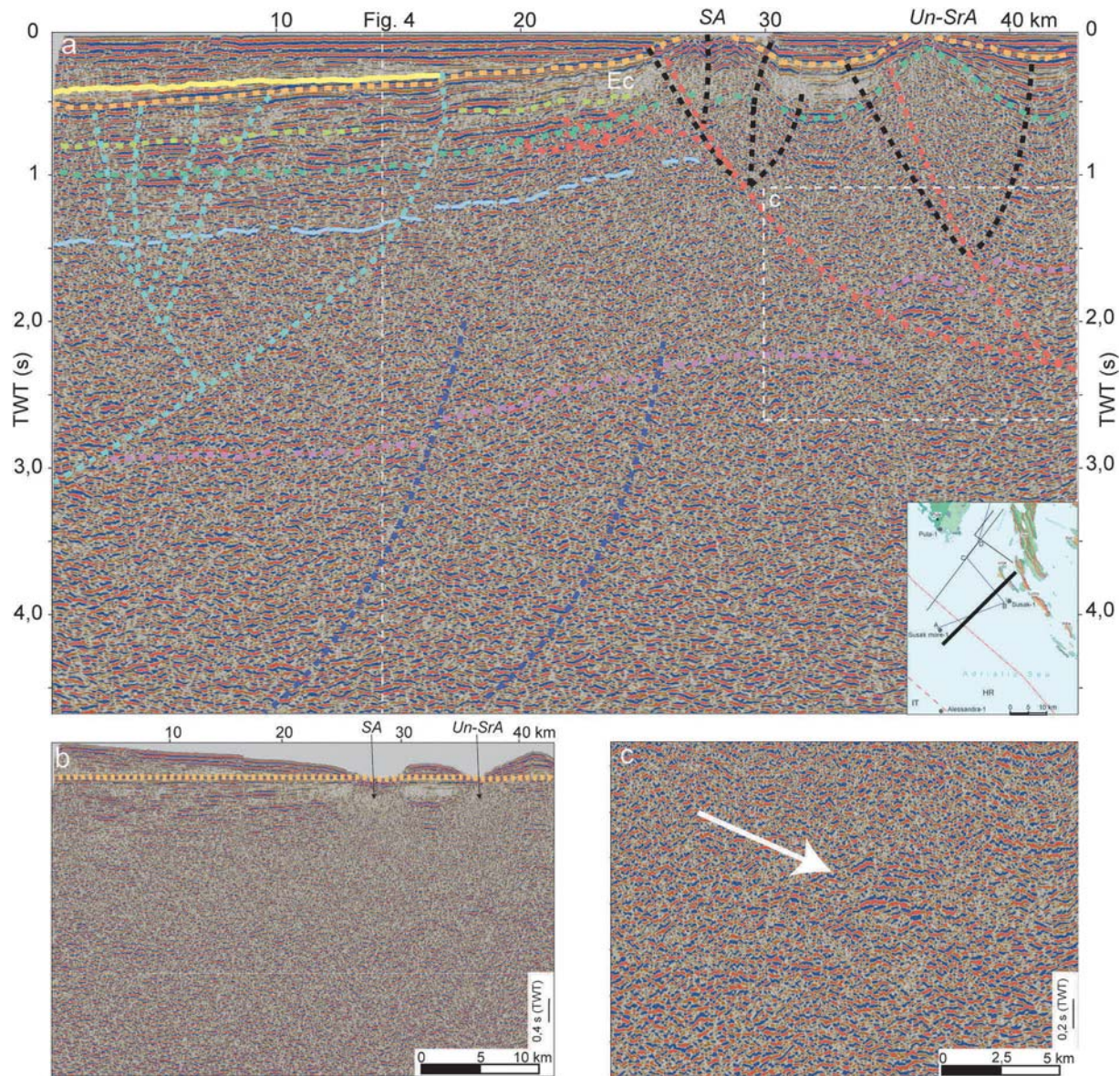
Fig. 8. Seismic profile through the Susak and the Unije-Srakane Anticlines. a) The left part of the profile shows the Pliocene tilting toward the Apennine Chain, which produced normal faults (light blue lines). Some of them likely reactivated the Triassic extensional faults (dark blue lines), generally affecting the deep Lower to Middle Triassic clastic sequence (below the pink horizon). The Susak and Unije-Srakane anticline structures (SA and Un-SrA) to the right were produced by Eocene thrusting (red lines) with syn-tectonic (Flysch?) strata (Ec). These structures were reactivated by post-Messinian transpressional deformation (black lines). We cannot exclude that they were originally isolated carbonate platforms. b) The section flattened on MES horizon gives an approximate image of the set-up in a post-Eocene compression/pre-foreland-tilting and Plio-Quaternary deformation time. c) White arrow indicates the faulted top of the Lower to Middle Triassic clastic sequence. (For interpretation of the references to colour in this figure legend, the reader is referred to the Web version of this article.)

shows low-frequency medium-to low-amplitude reflectors, which are continuous in the upper sequence and become discontinuous in the lower sequence, likely due to folding and fracturing. However, semi-transparent seismic facies in the infill of synclines or fronts of anticline structures was related to the flysch unit.

4.5. Carbonate platform (SFU4 and SFU5)

The top horizon is continuous and generally well defined by a parallel high-amplitude (due to the high average velocity of the platform) and low-frequency reflectors (Fig. 6 a). The typical carbonate platform facies is transparent and can be recognized along most of the profiles. Some transitional limestone units can be interpreted based on several low-amplitude reflectors, especially in the western part of the study area and in other restricted sectors, inside the shallow water carbonate

domain (e.g., between 20 and 35 km of the composite profile of Fig. 4).

4.6. Deep clastic sequence (SFU6)

The deepest sequence interpretable along the available seismic data is represented by a clastic sequence related to the Permo-Triassic rifting phase involving the Adria plate (Channell et al., 1979). The sharp contrast between the high velocity of the carbonate platform and the lower velocity of the clastic sequence produces a high-amplitude reflector (Fig. 7), already recognized as the base of the Dolomia Principale (horizon T in Del Ben, 2002) along the CROP-M16 profile, which represents the SW continuation of the composite profile of Fig. 4. This transition from the carbonate platform to the clastic sequence is characterized by a low-frequency seismic package, while it can be only rarely identified by its negative polarity seismic attribute. The lower sequence
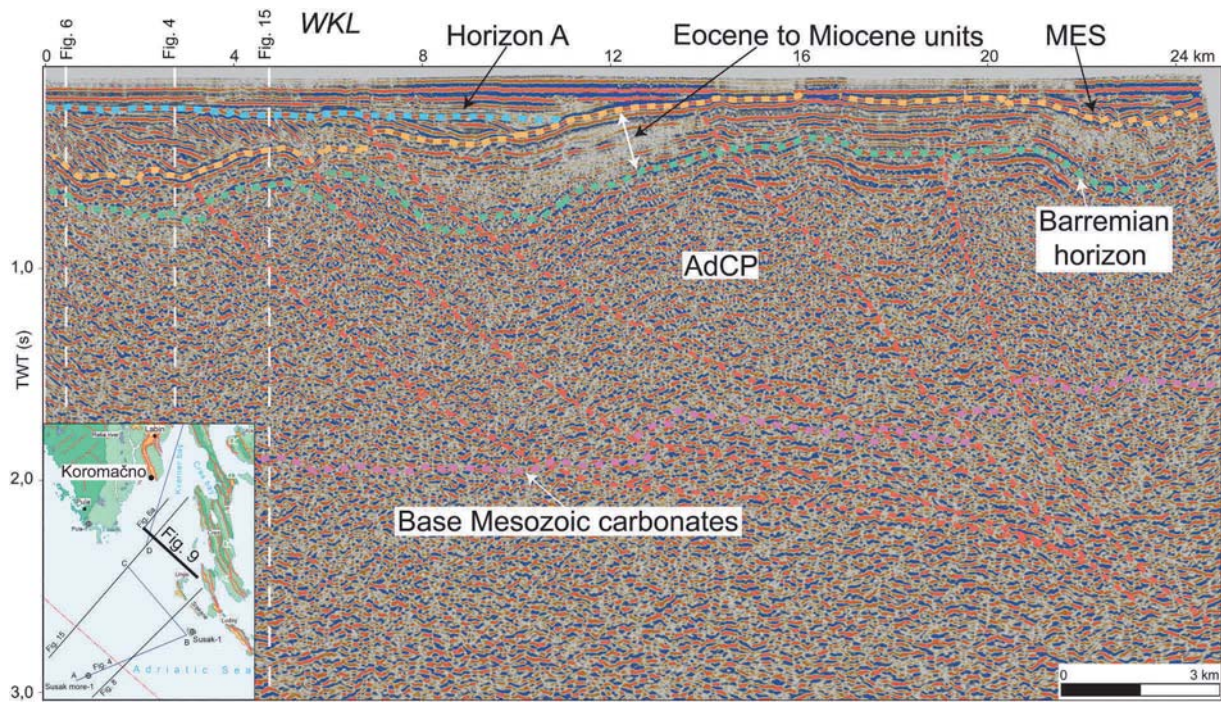
Fig. 9. Seismic profile crossing the W-Kvarner lineament. On the left, a clinoform system fills the channel downlapping to the MES. On the right, an Eocene thickness was interpreted, referred to as turbidite deposits of the Dinaric foreland. Thick-skinned tectonics was evaluated.

shows more discontinuous reflectors, due to the signal absorption at this depth and to the fracturing and tilting of several blocks during the main extensional tectonic phase (Fig. 4, 0–40 km). The bottom of the SFU6 unit is generally not identifiable along the profiles, so the thickness is unknown. Along the composite profile (but deeper than the maximum depth of Fig. 4), this basal reflector could be hypothesized at a depth of 4 s (TWT). If this is correct, we can evaluate a thickness of 2000–3200 m, likely lying directly on the crystalline basement (Fig. 7).

5. Results

The analysis of the available seismic and calibration data allowed us to interpret all the seismic, boreholes and surface datasets, as well as to construct the time structural maps of the MES and Lower Cretaceous horizon (AdCP).

5.1. Interpretation of seismic data

The main structures and their ages and geodynamic roles in the study area were distinguished by analyzing the relatively close-spaced grid of seismic profiles. The carbonate lithology of the AdCP influenced the seismic facies and deformational style of the area. The main Dinaric compressional tectonic phase caused the uplift of massive blocks along subvertical faults, rather than the typical plastic deformation usually affecting the pelagic sequences. In some cases, lithological differences or discontinuities represent decollement zones.

The composite profile in Fig. 4 illustrates the regional setting in the Kvarner area through differently oriented parts of several seismic profiles, from the Central Adriatic axis to the offshore area in the Rijeka Bay (Fig. 1).

We observed that the western study area, represented here in the profile between 0 and 37 km (Fig. 4), is tilted westward. Plio-Quaternary sediments reach over 500 m of thickness, as calibrated by the Susak more-1 well (Fig. 3).

The primary seismic marker is represented by the MES, which locally clearly truncates the peri-reef fossiliferous carbonates of Paleogene–lower Miocene layers (Susak more-1 well). It is the top of the

SFU3, which is highlighted by a seismic package of very high-amplitude reflectors (Figs. 4 and 5). Between 16 and 38 km, SFU3 becomes thicker while, between 67-74 and 95–112 km in Fig. 4, the Plio-Quaternary sequence (likely only Pleistocene, SFU1) directly covers the Cretaceous carbonates (SFU4) (Fig. 6). This long sedimentary hiatus (from Cretaceous to Pliocene) seems to be particularly related to a non-deposition due to a lowstand setting, emphasized by Messinian erosion.

Below the high-amplitude markers, the truncated carbonates are fractured and tilted by normal faults. They deform and cut the pre-MES sequence, testifying a Paleogene-Miocene activity, partially continued until Pliocene, as seems to be particularly evident for the normal fault at km 25 (Figs. 4 and 7). At a depth of 1.1–1.2. s TWT, Barremian limestones, calibrated by the Susak more-1 well, have been interpreted (Fig. 4); however, further eastward continuation from Kvarner and Cres Bay is below the seismic resolution of the composite profile. The AdCP shows opaque seismic facies, which are locally more stratified. Owing to the difficulty of recognizing the tectonic deformation on the weak seismic signals, we have only tentatively drafted some of the major faults. Generally, some gentle folding and local vertical offset suggest the presence of faults. Below the low-amplitude reflections of the carbonate platform, at a depth of 2.4 s TWT (5348 m at Susak more-1 well), a high-amplitude, low-frequency seismic package typically marks the top of the Lower to Middle Triassic clastic sequence. This sequence was encountered at 5235 m below sea level in the Alessandra-1 well (https://www.videpi.com/videpi/videpi.asp, Fig. 1), about 38 km to the south of the Susak-more 1 well, in the Italian offshore.

The deep seismic package of the Lower to Middle Triassic clastic unit, between 2.6 and 3.0 s TWT, is affected by normal faulting (blue faults in Figs. 4 and 8). Some of them were possibly reactivated during the Paleogene-Pliocene extensional tectonics discussed above. Toward NE, the profile of Fig. 8 ends near Lošinj Island: it crosses the northwestern extension of the Susak (SA) and Unije-Srakane (Un-SrA) highs. Both appear to be symmetric (at least in the NE–SW direction of the profile) and onlapped by deformed sediments. This suggests, as alternative hypothesize, their possible origin as isolated carbonate platforms, likely developed until Late Cretaceous or early Paleogene, that were successively tectonically deformed. We ascribe the opaque seismic sequence
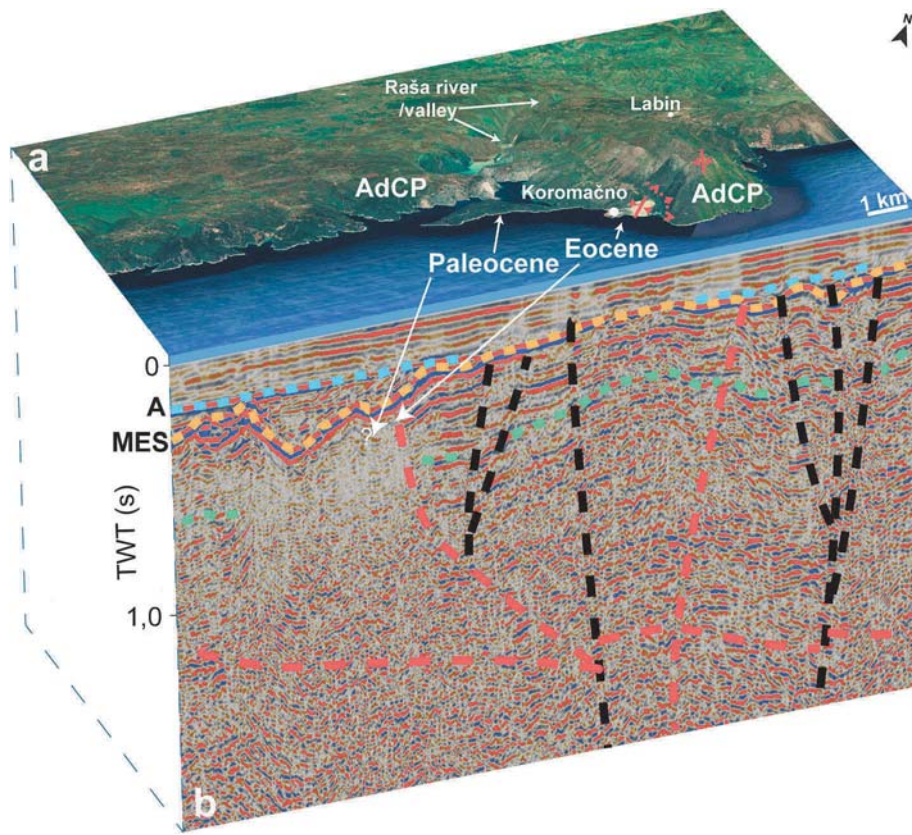
Fig. 10. Surface (a) to subsurface (b) correlation of major structures in the Koromačno-Labin outcrop area (position in Fig. 1): the structure continues in the western Cres Anticline.

below the MES, reaching a thickness of 400 ms TWT, to an Eocene age. The same sequence was also interpreted to the SW of the Susak Anticline (23–26 km in Fig. 8). Moreover, to the north of the Unije-Srakane Anticline, a grow stratum marks the pre-Messinian syn-tectonic deposition (37–43 km in Fig. 8). The Pleistocene sequence covers both the structures horizontally, onlapping the folded MES.

The high-amplitude low-frequency Lower to Middle Triassic folded reflectors are evident at a depth of 1.7–2.2 s TWT in the NE part of section. A pull-up seismic effect unavoidably emphasizes this deep anticline. However, its shape and position allow us to hypothesize that the Lower to Middle Triassic clastic deposits are involved in thrusting deformation (Fig. 8c). To explore the tectonic features that produced the uplift of the two anticlines during the pre-Pliocene, we unfolded the MES reflector to eliminate the effect of the Plio-Quaternary uplift (Fig. 8b) and the westward tilting of the crust due to the loading of the Apennines. This is not a restoration to the Miocene situation as it does not consider the Messinian erosion (which, if present, is below the seismic resolution) and the horizontal component of deformation. Nevertheless, it provides a reasonable approximation of the pre-Pliocene geological setting, evidencing the two structures composed of AdCP carbonates separated by a pre-Messinian basin. This is filled by a semi-transparent sequence that is also present in the SW of the Susak Anticline.

In Fig. 4, at 39–46 km, the structural high of the Susak Anticline evidences a deformed MES, representing an effect of the Plio-Quaternary outermost deformation in this area. Toward the NW, the anticline limits a large area (approximately 50 km in Fig. 4) of erosional truncation.

The positive structure at 66–73 km in Fig. 4 is a marginal part of the southern Istrian Swell structure, which is completely buried below the Pleistocene sediments. It is crossed by two orthogonal transects of the composite profile (position in Fig. 1). MES truncates the pre-Messinian units and shows a planar surface. On the eastern sides of this structure, a canyon system is evident between 50 and 66 km and between 74

and 94 km. Both are part of a W-Kvarner lineament bordering the eastern side of the Istrian Swell. The system is filled by a sedimentary unit that is probably partially clastic, as testified by clinoform geometry with variable amplitude and by reflector continuity. From 70 to 138 km, the composite profile remains parallel to the eastern Istria shoreline, characterized by a steep coast, cut by several deep valleys continuing in the offshore structures, as evidenced in the profile.

A prograding clinoform system, with opposite vergences (apparent direction along this profile), filled these valleys. Clinoforms are especially evident between 74 and 94 km, between 112 and 155 km of Fig. 4, and in the intermediate syncline between the SA and Un-SrA in Fig. 8. The NW–SE profile of Fig. 9 crosses orthogonally to the Istrian coast. The clinoform system downlaps in the SW direction of the Cenozoic seismic package topped by the MES. This package is cut by compressive/transpressive faults and covers an opaque seismic sequence ascribed to Eocene formations.

The upper part of the clinoform deposits toplap an erosional surface ("A"), which is parallel to the overlying Pleistocene unit and is characterized by medium/high-amplitude reflection (Figs. 4, 6 and 8). More than an erosional truncation, the A reflector represents a topset unit consisting of nearly horizontal layers, often below the seismic resolution, representing proximal deposition (Catuneanu, 2006).

Between 94 and 115 km (Fig. 4), a buried high structure was interpreted in all the profiles between the onshore Labin–Koromačno structure (Fig. 10) and the western Cres Anticline (Fig. 1). The MES remains sub-parallel to the underlying pre-Pliocene layers, while the Pleistocene deposits show semi-transparent seismic facies and eastward onlapping terminations. Below the first multiple ("m" in Fig. 4) of the MES reflector, the seismic signal becomes very poor.

In the whole composite profile between 112 and 152 km, the MES reflector highlights deep valleys filled by sedimentary units with clinoform geometries. This leads us to two important observations: i) the MES
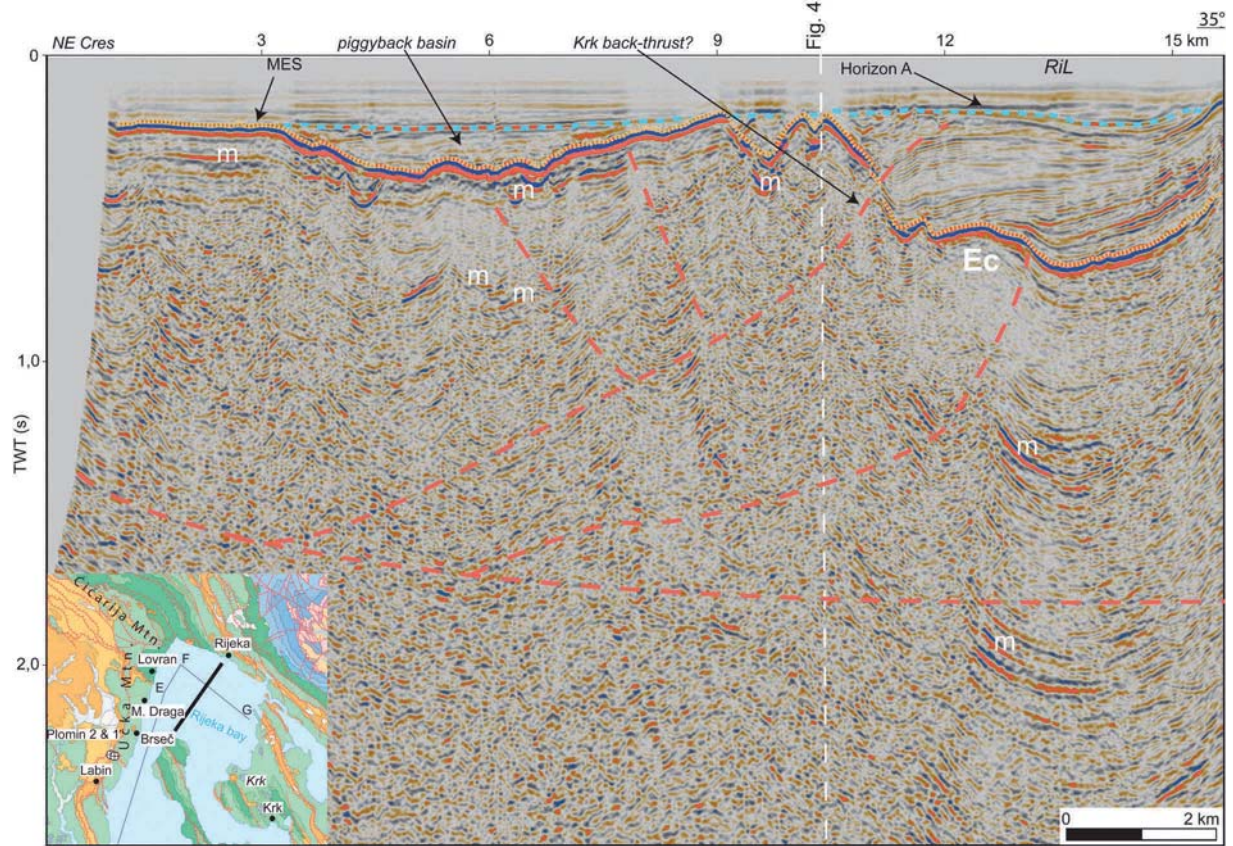
Fig. 11. Seismic profile with SW–NE direction, from the Cres to the Rijeka coasts. A deep basin is present between the Rijeka coast and the Krk back-thrust. The valley between 3 and 9 km is filled by a clinoform system downlapping the high amplitude reflector of the MES. The MES shows only a weak angular relationship with the underlying layers testifying that erosion clearly developed in the piggy-back basin. The deeper red dashed line, representing a SW verging thrust, has been interpreted on several profiles of the seismic dataset, as also in the northern part of the composite profile of Fig. 4. To the SW, the Cres offshore shows a sub-horizontal setting. (For interpretation of the references to colour in this figure legend, the reader is referred to the Web version of this article.)

does not show a clear erosional truncation; ii) generally, the pre-Messinian low-amplitude reflectors show to be parallel to the MES reflector below both the structural highs and lows.

The eastern part of the composite profile (between 142 and 162 km) has a NW–SE direction, parallel to the Rijeka shoreline. The high-amplitude continuous MES reflector in the northwestern low structure is parallel to the underlying low-amplitude reflectors. It is also onlapped by the discontinuous clinoform system, upward truncated by "A" and covered by the horizontal Pleistocene sequence. This confirms homogeneous depositional environments in the entire Kvarner area.

In Fig. 11, a NE–SW oriented profile better depicts the tectonic structures of Rijeka Bay. The Krk structure seems to originate from back-thrust activated above a deep NE-verging thrust system and deforming sediments immediately underlying the reflector A 11–12 km. Moreover, the piggy-back basin between 3 and 9 km is filled by tilted, partially SW-ward prograding deposits onlapping the MES.

A deep basin (base at a depth of 0.7 s TWT, more than 700 m thick, considering an average P-velocity of more than 2000 m/s) separates the submerged northwest anticline of the Krk Island from the onshore Dinaric orogen. The basin has been filled by SW deepening layers, onlapping the MES and tilted by an uplift of the northeastern structure, as evidenced at the NE end of the profile. Internal growth strata imply that this uplift was coeval to the infilling deposition and continued more recently. The horizontal reflector A is gently deformed, and it truncates the basin fill which is covered by Pleistocene deposits. The deep opaque seismic facies below the MES (5–7 km and 11–13 km) suggests the presence of Eocene flysch involved in late Dinaric compression.

5.2. Time structural maps

Time structural maps of the MES and the AdCP horizon have been produced to highlight the structural pattern of the study area. The two maps clearly differ in deformation events that took place after the AdCP deposition and before the Messinian erosional event, indicating that they vary in the critical effect of Eocene Dinaric deformation. At the same time, their comparison allows us to distinguish the impact of the Messinian event and analyze its relationship with the previous deformation.

5.2.1. Time structural map of a Lower Cretaceous horizon

We decided to interpret and map a horizon within the Lower Cretaceous carbonate sequence because of its better visibility than other reflectors present below the Cenozoic sequence. The achieved map (Fig. 12) is limited to the west of Cres Island because deep seismic reflectors are scarce in the northeastern part. On the other hand, we found it useful to compare the maps of the MES and of this deeper reflector. As the eastern slope of the Istrian Swell, the SW slope of the Susak Anticline is also emphasized by the tilting effect of the Apennine foreland towards the west. The WKL is more than 850 ms TWT deep. The Lower Cretaceous horizon map shows the Susak Anticline, bordered by steep slopes, both in the SW (Figs. 4 and 8) and NE (Fig. 8) sides.

5.2.2. Time structural map of MES

This map (Fig. 13) regionally highlights the same primary structural highs and lows of the MES. The main seismic marker in the Mediterranean Sea is generally the base of the Plio-Quaternary sequence. It is
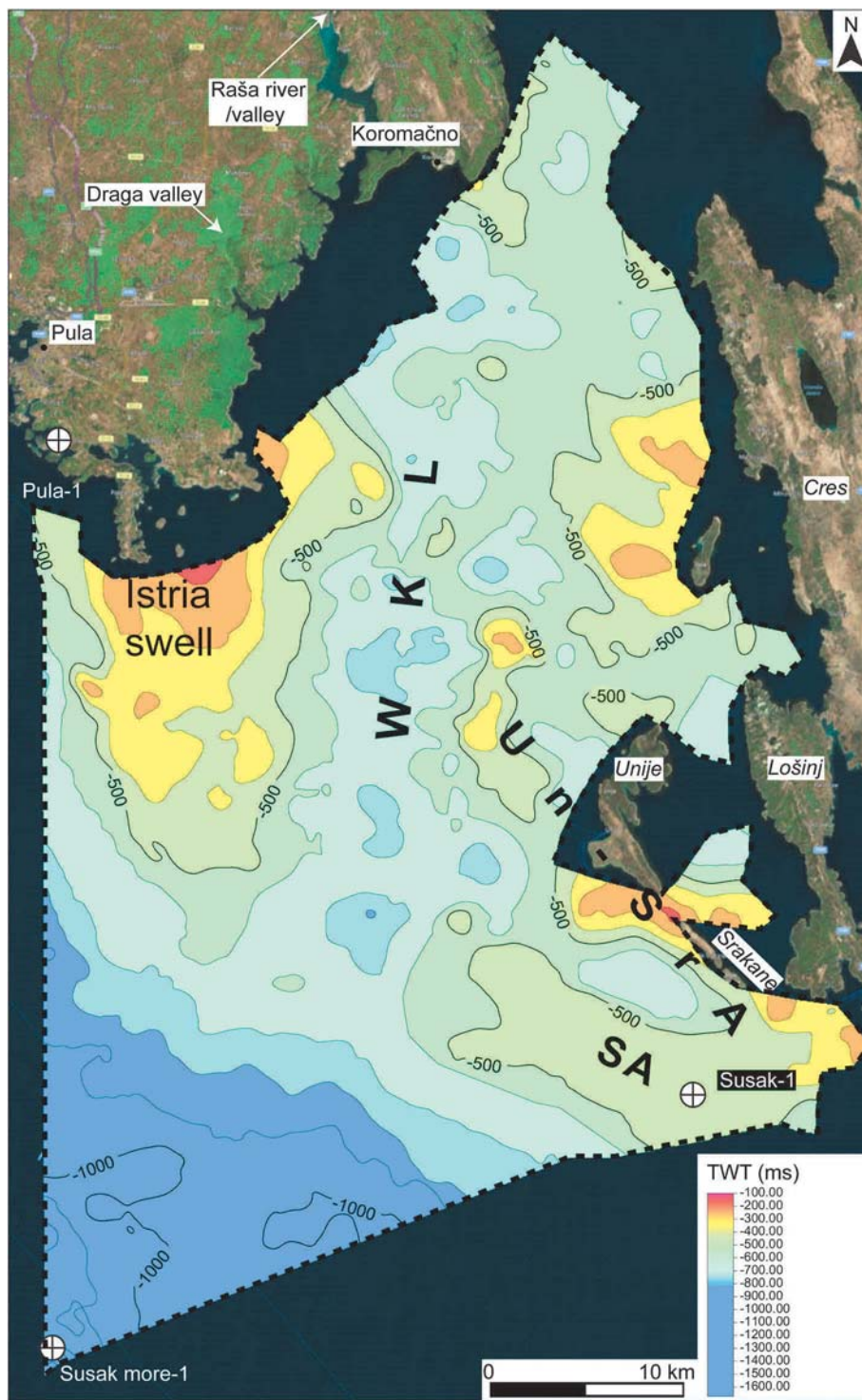
Fig. 12. Time structural map of the Barremian horizon, within the Lower Cretaceous carbonates. SA: Susak Anticline, WKL: West Kvarner lineament, Un-SrA: Unije-Srakane anticline.

caused by the Messinian event, known as the Messinian Salinity Crisis (MSC), related to a decreasing sea level (Hsü et al., 1978; Lofi, 2018), which caused two main effects: i) on the continental margins, it caused the emersion of the continental slopes and following erosional truncation (MES), locally emphasized by the presence of canyons in the sea bottom and valleys in the alluvial plains; ii) in the basins, it generated favorable conditions for gypsum precipitation (Gessoso Solfifera Formation), and in the very deep/oceanic basins, the deposition of enormous volumes of salt.

In Rijeka Bay, the MES often reached Cenozoic carbonate ramp deposits and locally the Mesozoic carbonate platform. Both erosion and evaporite deposition generally determine a sharp difference in the acoustic impedance between the overlying Plio-Quaternary sequence and the underlying Messinian or pre-Messinian sequences, with the result of a high-amplitude reflector.

In Fig. 13 the MES time structural map, obtained from interpretation of the available seismic profiles, from SW to NE, depicts the following major structural features:
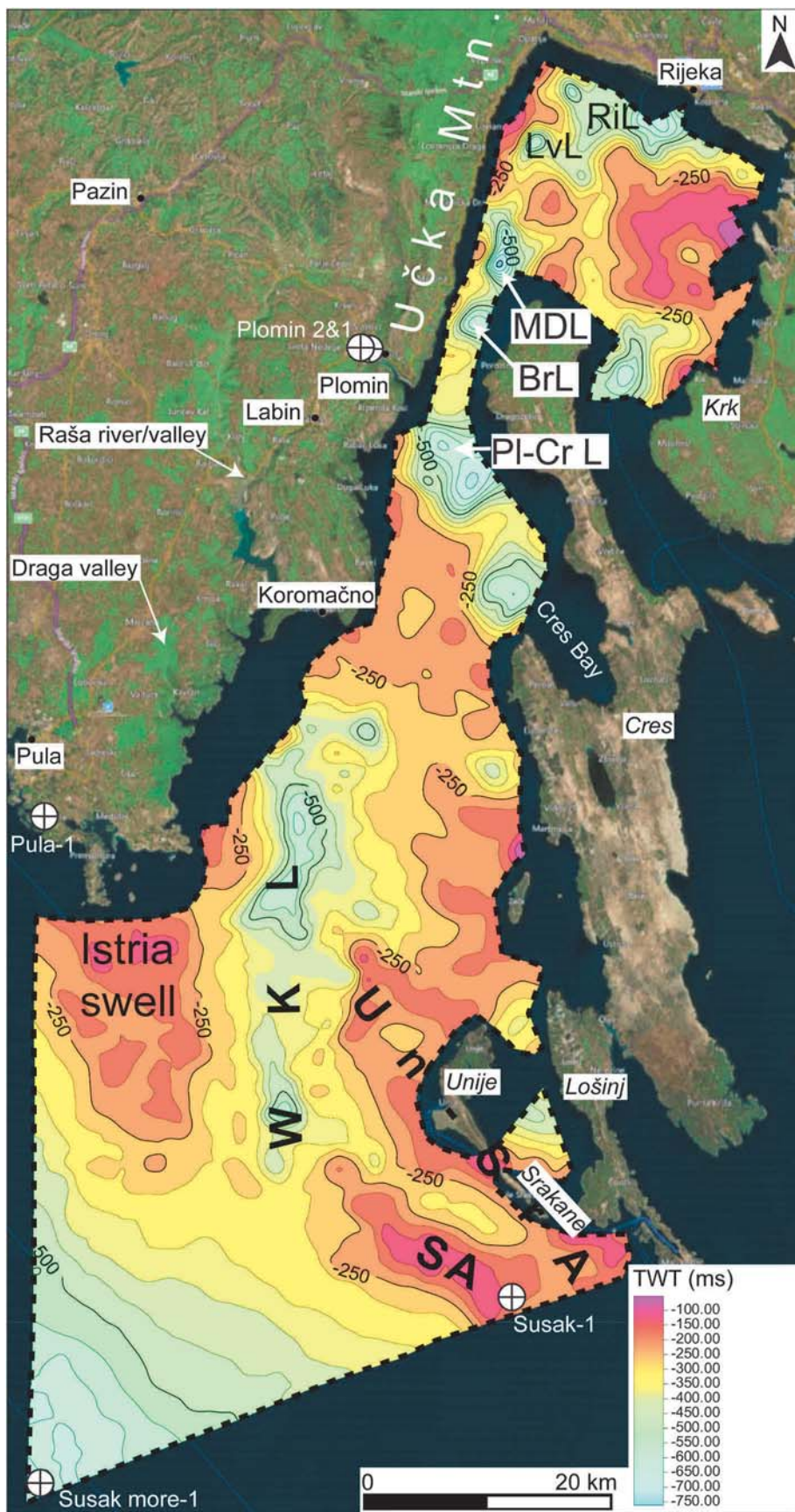
Fig. 13. Time structural map of the Messinian erosional surface. **SA:** Susak Anticline, **WKL:** West Kvarner lineament, **Pl-Cr L:** Plomin-Cres Bay lineament, **BrL:** Brseč low, **MDL:** Mošćenička Draga low, **LvL:** Lovran low, **RiL:** Rijeka low.
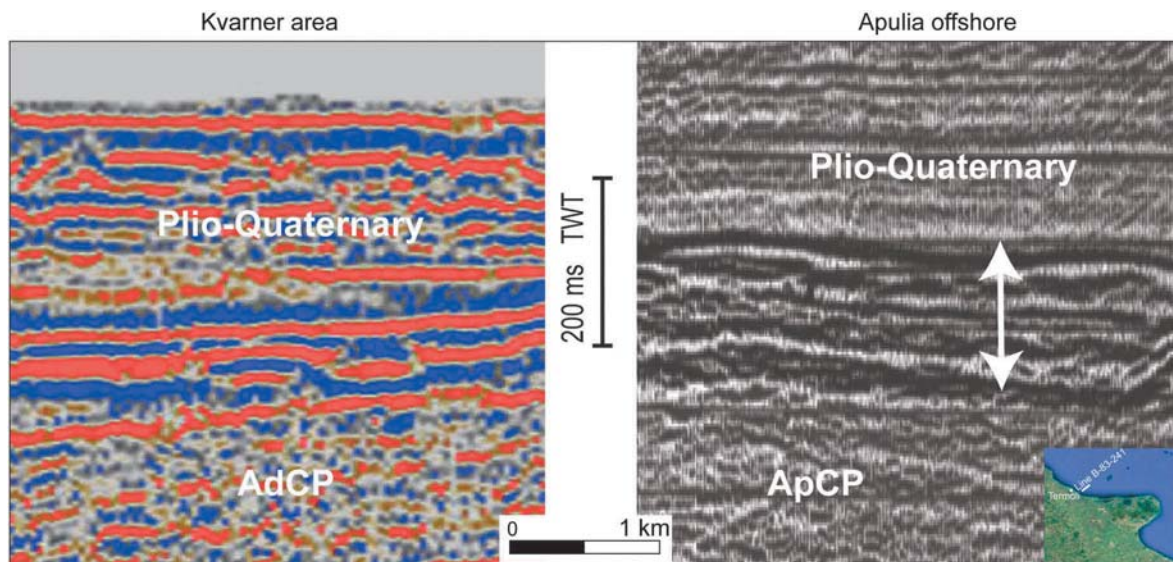
Fig. 14. Seismic facies a) in the Kvarner Area (detail from Fig. 4) and b) in the Central Adriatic Sea (details from Line B-83-241, calibrated by the Cristina-1 well and present in https://www.videpi.com/videpi/videpi.asp). The high-amplitude seismic package, highlighted by the white arrow, is composed of 156 m of Messinian gypsum and 118 m of deep carbonate of Schlier and Bisciaro Formations, overlying the Apulia Carbonate Platform (ApCP). Comparison suggests that the presence of gypsum evaporite cannot be locally excluded, as also here in the Kvarner area.

- The southwestward deepening in the SW sector is caused by the Plio-Quaternary migration of the Apennine Chain. This feature is the farthest effect of the Apennine foreland tilting.
- The southern extension of the Istrian Swell (Fig. 4, 66–75 km; Fig. 13) and the western extension of the Susak Anticline are depicted. They are separated by a series of relative lows, called "W-Kvarner lineament" (WKL), which continues inland the Istria Peninsula in the Raša Valley.
- The map is generally truncated around the shorelines, due to a shallower MES which disappears in the upper part of the profiles.

- A structural high system connects the Labin-Koromačno onshore structure with the Unije-Srakane, Lošinj and Cres anticlines.
- The structural low of Cres Bay continues in the Plomin Valley of the Istria Peninsula, which separates the Labin-Koromačno anticline and Učka Mountain.
- Several filled valleys in the northernmost part of Kvarner Bay (Fig. 4, 117–137 km) are in the southeast continuation of the onshore valleys orthogonally cutting the Učka structure (Fig. 1).
- The Krk anticline extends toward the NW (Fig. 4, 147–162 km) sitting on the back-thrust shown in Fig. 11, while the northeastern
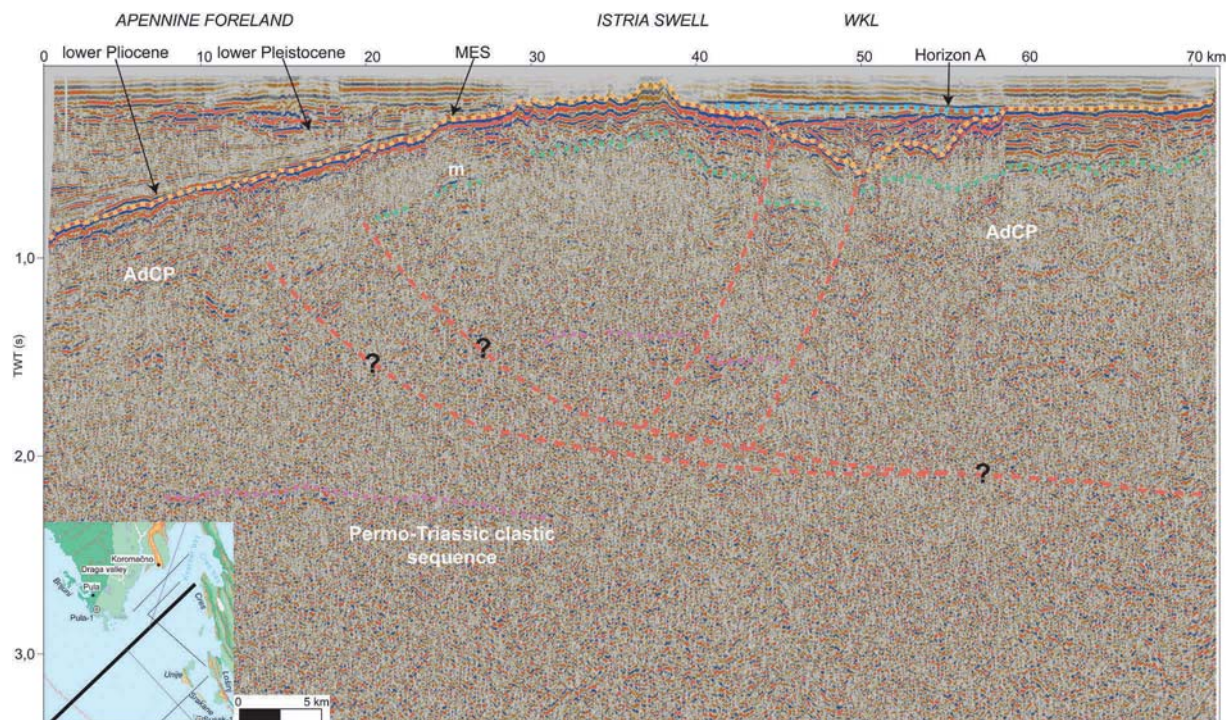

Fig. 15. Seismic profile crossing the southern offshore Istria Swell, here interpreted as related to compressive tectonics. The western side is emphasized by the westward tilting of the Apennine foreland.

15

foredeep basin separates the island from the structure uplifted in the Rijeka onshore.

6. Discussion

In the study area, evidence of the Plio-Quaternary deposits onlapping the MES reflector to the east, testifies the Adriatic foreland post-MSC tilting toward the Apennine frontal thrust. This occurred until the early Pleistocene (Fig. 5), as the last effect of the regional Pliocene tilting, documented in the Italian Adriatic offshore by the CROP-M16 profile (Del Ben, 2002). Some normal faults that cut or deform the MES, are joined to the tilting, sometimes reactivating older normal faults that affected the deeper Lower to Middle Triassic clastic sequence. A pre-Messinian fault activity seems to be related to the NE–SW-oriented minimum paleostress axis, interpreted by Žibret and Vrabec (2016) in Slovenia onshore, as an expression of the Early to Middle Miocene back-arc extension in the Pannonian Basin system. Also along the wider Rijeka area shoreline, Palenik et al. (2019) interpret a change in the regional stress field during the Neogene-Quaternary.

To the southwest of the Susak Anticline, the Paleogene to Miocene seismic package becomes thicker than in the Susak more-1 well (Figs. 4 and 8) owing to the effect of the Susak Anticline uplift and to the Messinian erosion. Here, the seismic facies suggest the presence of Messinian evaporite, which is otherwise not found in wells in the Northern Adriatic Sea. The reflection signatures in the pre-Pliocene seismic package of the Kvarner area are very similar to those seen in profiles in the Central Adriatic Sea, where gypsum has been confirmed, as shown in Fig. 14.

Toward the east, several anticline and syncline structures alternate in Kvarner Bay. They developed by deformation of the AdCP during Dinaric orogenic phase and following Neogene tectonics. To the west of the study area, the transition between the shallow-water domain of the AdCP and deep marine domains of the Umbria-Marche basin is highlighted by the CROP-M16 (Del Ben, 2002) and other profiles in the central part of the Adriatic Sea (Grandić et al., 1999; Fantoni and Franciosi, 2008).

The first prominent structure of the study area is represented by the southern extension of the Istrian Swell; its southwestern side was emphasized by the westward tilting of the Adria. Matičec et al. (1996) analyzed the relationship between the spatial occurrence of Eocene Foraminifera Limestones and the different stratigraphic levels of Cretaceous carbonates in the Istrian part of the AdCP. They concluded that since the Lower Cretaceous, several tectonic phases contributed to the Istrian Anticline uplift. The available seismic profiles do not clearly show the deep thrust, but we cannot rule out their presence, particularly in the profile of Fig. 15, in which some weak NE-dipping reflectors suggest their possible position. Moreover, two interpreted back-trusts, separating the Istrian Swell from the W-Kvarner lineament, have also been reactivated with positive inversion tectonics during the Eocene compressional phase. The east-verging thrust is cut by two segments of the composite profile, which are reciprocally orthogonal (40–72 km and 72–80 km in Fig. 4) and bound the Istrian Swell toward the east. A higher structural level of the Triassic clastic sequence was also hypothesized by to SW of the northern Dalmatian Islands. Furthermore, to the west of the Istria Peninsula, the gravity map from Grandić et al. (2001) shows the maximum value of the Bouguer anomaly, which is possibly correlated to a basement higher structural position (Grandić et al., 2001; Wrigley et al., 2014).

The Susak, Unije-Srakane, Lošinj, Cres, and Krk Anticlines developed during the Eocene orogenic phase of the Dinarides. Syn-tectonic strata, recognized in the growth wedge between or in front of anticlines (Figs. 4 and 8–10), testify to the pre-MES age of this compressional deformation. The wedge has been tentatively ascribed to the flysch unit or its proximal equivalent carbonate/Jelar breccia, recognized in the central External Dinarides (Tari Kovačić and Mrinjek, 1994; Korbar et al., 2010; Tomljenović et al., 2018; Vlahović et al., 2018) and Krk Island (Korbar, 2009).

In particular, the strike of the Susak Anticline axial surface is in a NW–SE direction, as shown in the orthogonal profiles of Figs. 4 and 8, and in the time structural maps (Figs. 12 and 13). The SA and the Un-SrA have been interpreted as originating from Eocene thick-skinned tectonics, suggested by deformation of deep horizons of the Lower to Middle Triassic clastic sequence. As mentioned previously, an intermediate basin filled by a syntectonic sedimentary sequence is ascribed to the Eocene flysch and carbonate/Jelar breccia units. The two symmetric anticlines have been attributed to positive flower structures, reactivating the older thrust. This transpressive neotectonics occurred after the MES and before the formation of the Pleistocene unconformity "A". This represents a regional sub-horizontal marker, likely related to a Pliocene–lower Pleistocene (?) topset unit.

The WKL is represented by an alternation of structural highs and lows between the eastern Istria coast and the Cres, Lošinj and Unije Islands. Structural lows are filled by deposits with mostly clinoform geometries downlapping the MES. They represent the offshore continuation of incised synclines, which cut the hilly reliefs of the Istria shoreline and affect island morphology.

More frequently, these valleys are based on the MES, approximately conformable to the underlying low-amplitude reflectors. This suggests an important post-MES deformation phase, which controlled the position of the channels, canyons and valleys. This is also confirmed by a comparison between the structural maps of the Lower Cretaceous carbonate and the MES (Figs. 12 and 13). In both maps, the N–S trending depression along the WKL is clearly recognized.

The Lower Cretaceous carbonate is only locally reached by the Messinian erosion (Fig. 4). We can argue that the Kvarner valleys show a tectonic origin caused by the Dinaric orogen. These pre-MES compressional structures focused the Messinian erosion and were re-activated by the post-Messinian transpressional tectonics. Rivers such as the paleo Raša caused relevant erosional processes in the outcropping regions, taking away significant volumes of the pre-existing sedimentary sequence, especially Flysch deposits.

The high-amplitude reflector MES, corresponding to the main regional unconformity, is often coincident with the unconformity "A." The MES is tectonically folded in the Istrian Swell's offshore extension, Susak and Unije-Srakane Anticlines, S-Labin-Koromačno, NW-Krk Anticlines and Rijeka onshore Anticline (Figs. 4, 8–11 and 14).

MES is covered by the downlapping deposits of the prograding sequence, likely related to a fluvial drainage pattern. The evidence of offlap at the top, related to the reflector "A," indicates a change from sedimentation to erosional event: it marks a transgression after which the Pleistocene marine environment established.

These clinoform infilling deposits, never calibrated by wells, can be ascribed to an early Pliocene deposition, possibly as re-sedimented deposits originating from a prograding system from today's inland areas (Istria and wider Rijeka region). As an alternative hypothesis, we can consider the latest Messinian (or last Messinian/early Zanclean, in agreement with Do Couto et al., 2014) post-evaporitic Lago Mare unit to be present in several places in the paleo-Mediterranean domain (Lofi, 2018), which is mainly composed of a conglomerate of alluvial fans or lacustrine marl overlaying a main erosional surface (Do Couto et al., 2014; Cornee et al., 2016). Several wells penetrated this sequence in the western Adriatic Sea. Furthermore, similar geometries were found in outcrops of the northern Apennines (Fig. 6). Some primary analogies, corroborating the idea about a Late Messinian age of the infilling sediments of the Kvarner area, can be recognized:

1. A relevant unconformity at the base
2. A typical depositional setting of a continental/shallow water domain
3. A medium/high-amplitude reflector at the unit top, corresponding to the abrupt lithological transition from the Lago Mare deposits to the overlying marine deposits
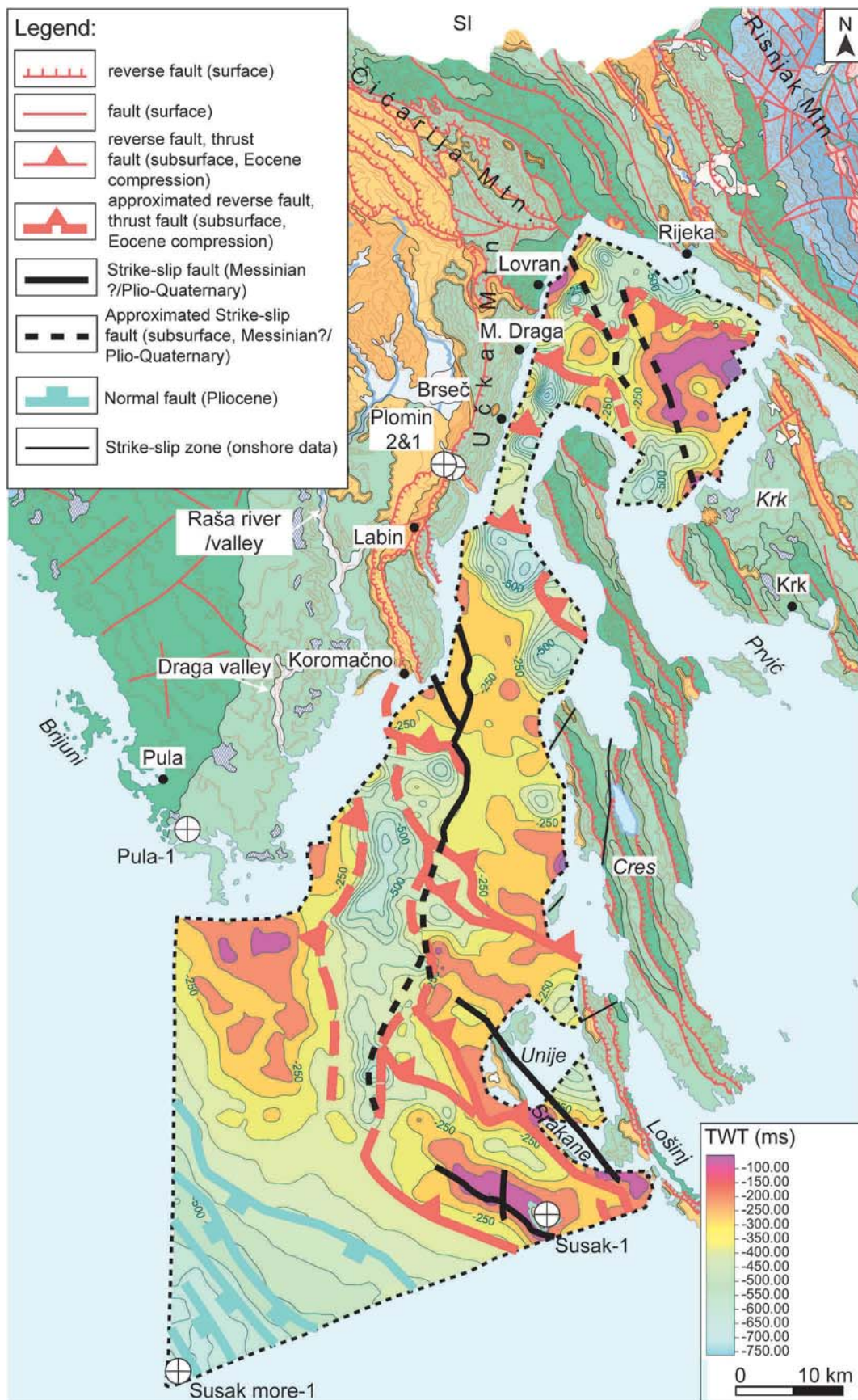4. The overlying sub-parallel Plio-Quaternary layers

Fig. 16. An attempted correlation between onshore and offshore main faults on the MES structural map in the Kvarner area (onshore data from GKRH, 2009; Fuček et al., 2012; Fuček et al., 2015). Red lines are pre-MES thrust faults, black lines are Pliocene–early Pleistocene transpressive systems, often reactivating the previous thrust. (For interpretation of the references to colour in this figure legend, the reader is referred to the Web version of this article.)

The Mid-to Lower Triassic clastic sequence involvement in faulting has been evidenced below both the offshore Labin-Koromačno and Unije-Srakane anticlines. Both belong to the same structural high system crossing Kvarner Bay in the NNW–SSE direction (Fig. 12) that seems to originate from Eocene compressive tectonics reactivated by post-MES transpression.

The pre-Messinian compressive faults have been mapped (red lines in Fig. 16), showing a predominately NW–SE direction. They represent the more external part of the Eocene Dinaric thrust system. During the Pliocene–early Pleistocene, a transpressive deformation (black lines) affected the area, often reactivating pre-existing structures. These recent tectonics seem to be weakly rotated with respect to the previous one, and structures have assumed a main NNW–SSE direction. We also hypothesize that the Istrian Swell could have played an essential role in distributing the stress field of the region, partially hindering the westward propagation of the Dinaric thrust system.

7. Conclusions

- The Kvarner area is dominated by an alternation of structural lows and highs, mainly oriented:
1. N–S in the Istrian Swell and in the north–south trending lineament of structural lows (here called West Kvarner lineament, WKL) and in the southern Rijeka Bay;
2. NNW–SSE in the Krk, Plomin-Cres Bay, and northern Lošinj Islands;
3. NW–SE in the Susak, Unije/Srakane and Southern Lošinj anticlines and the Rijeka Bay.

Deformation is characterized by a mix of thin- and thick-skinned tectonics. The thrust structures, which originate from compressive and transpressive deformation, are also affected by the resistance of the thick AdCP deposits. Deformation often involves the Mid-to Lower Triassic clastic sequence and possibly the underlying crystalline basement. The compressional tectonics produced significant vertical displacements, while small horizontal displacement appeared to be present, particularly in the western, less deformed sector of the Kvarner area.

The Eocene to Miocene unit covers the AdCP succession, only weakly truncated by the Messinian erosional event. This event is typically well expressed by a high-amplitude reflector, defined as the MES. Locally, some canyons incised to the level of the upper part of the AdCP deposits. Based on seismic facies and thickness of the Eocene/Miocene sequence, the presence of the Gessoso Solfifera Formation has also been hypothesized in front of the Susak anticline, locally covering the Eocene foredeep sedimentary sequence (SFU3). Some prominent tectonic structures testify to the post-MES deformation, principally symmetric anticlines. They suggest recent transpressional tectonics, often re-activating older compressive faults. Notably, the post-MES uplift of the anticlines affects their previous Eocene foredeep and confirms the role of the Eocene foreland thrust belt system in the development of the more recent (Pliocene/early Pleistocene) transpressive activity.

- The southern offshore continuation of the Istrian Swell is marked by an anticline structure related to a regional uplift by the Dinaric outermost compressional system. Due to the scarce reflectivity of the AdCP succession, deep Cretaceous (?) SW verging thrust faults, probably involving the Lower Triassic clastic, can only be hypothesized. The western side of the Istrian Swell is strongly emphasized by the Pliocene westward tilting of the Adria foreland toward the Apennine Chain. The tilting produced post-Messinian normal faults, often reactivating previous extensional faults. Gradually eastward younger Pleistocene layers onlap the tilted foreland. The eastern side of the Istrian Swell is affected by back-thrusts: they seem to have been active also in recent times.
- The north–south WKL lineament of structural lows is particularly evident in the MES time structural map. The morphology produced by tectonic deformation affected the Messinian water flow, with

consequent erosional and depositional effects. Toward the north, the WKL continues in the Raša Valley, penetrating several kilometers in the Istria Peninsula. Furthermore, the structural low of Cres Bay continues in the Istria Peninsula with the Plomin Valley, separating the Labin-Koromačno anticline and the Učka mountain.

- The anticline of Krk Island extends offshore toward NW, where it shows a back-thrust structure. It is separated from the Rijeka onshore by a deep Pliocene basin filled by deposits which downlap the MES reflector toward SW.
- Generally, a prevailing NW–SE strike of structures seems to characterize the Eocene thrust system. The Istrian Swell probably influenced the transpressional system developed to its eastern side, which partially reactivated the previous faults after the Messinian erosional event.
- The low structures evidenced in the MES map are filled by discontinuous, often prograding reflectors, generally offlapping to a shallower horizontal reflector ("A"). This filling sequence, never calibrated by wells, has been interpreted as alluvial to lacustrine deposition sourced from onshore areas. Its age is likely Plio-Quaternary; an alternative hypothesis suggests that it may be related to the Lago Mare Formation, deposited in the latest Messinian, after the erosional event. In the structural highs, emersion and corresponding hiatus were maintained throughout the Pliocene and likely early Pleistocene time.

Credit authors statement

Marko Špelić: Conceptualization; Data curation; Formal analysis; Investigation; Methodology; Project administration; Resources; Software; Supervision; Validation; Visualization; Writing – original draft, Writing – review & editing. Anna Del Ben: Corresponding author; Formal analysis; Investigation; Methodology; Supervision; Validation; Visualization; Writing – original draft, Writing – review & editing. Krešimir Petrinjak: Visualization, Formal analysis, Investigation

Declaration of competing interest

The authors declare that they have no known competing financial interests or personal relationships that could have appeared to influence the work reported in this paper.

Entrepreneurship and Crafts.

Appendix A. Supplementary data

Supplementary data to this article can be found online at https://doi.org/10.1016/j.marpetgeo.2020.104857.

References

Accaino, F., Busetti, M., Böhm, G., Baradello, L., Affatato, A., Dal Cin, M., Nieto, D., 2019. Geophysical investigation of the Isonzo Plain (NE Italy): imaging of the dinaric-Alpine chain convergence zone. Italian J. Geosci. 138, 202–215. https://doi.org/10.3301/IJG.2019.01.

Babić, L., Kučenjak, M.H., Ćorić, S., Zupanič, J., 2008. Evolution of a river-fed foreland basin fill: the North Dalmatian flysch revisited (Eocene, Outer Dinarides). Nat. Croat. 17, 357–374.

Bada, G., Grenerczy, G., Tóth, L., Horváth, F., Stein, S., Cloetingh, S., Windhoffer, G., Fodor, L., Pinter, N., Fejes, I., 2007. Motion of Adria and ongoing inversion of the Pannonian Basin: seismicity, GPS velocities, and stress transfer. Spec. Pap. Geol. Soc. Am. 425, 243–262. https://doi.org/10.1130/2007.2425(16).

Bennett, A.R., Hreinsdóttir, S., Buble, G., Bašić, T., Bačić, Ž., Marjanović, M., Casale, G., Gendaszek, A., Cowan, D., 2008. Eocene to present subduction of southern Adria mantle lithosphere beneath the Dinarides. Geology 36, 3–6. https://doi.org/10.1130/G24136A.1.

Bergant, S., Tišljar, J., Šparica, M., 2003. Eocene carbonates and flysch deposits of the Pazin basin. In: Vlahović, I., Tišljar, J. (Eds.), Field Trip Guidebook, 22nd IAS Meeting of Sedimentology - Opatija 2003, pp. 57–63.

Bigi, G., Cosentino, D., Parotto, M., Sartori, R., Scandone, P., 1992. Structural model of Italy. Scale 1:500,000. Quad. Ric. Sci. 114 (3).

Brancolini, G., Civile, D., Donda, F., Tosi, L., Zecchin, M., Volpi, V., Rossi, G., Sandron, D., Ferrante, M.G., Forlin, E., 2019. New insights on the Adria plate geodynamics from the northern Adriatic perspective. Mar. Petrol. Geol. 109, 687–697. https://doi.org/10.1016/j.marpetgeo.2019.06.049.

Brčić, V., Glumac, B., Fuček, L., Grizelj, A., Horvat, M., Posilović, H., Mišur, I., 2017. The cenomanian–turonian boundary in the northwestern part of the adriatic carbonate platform (Ćićarija Mtn., Istria, Croatia): characteristics and implications. Facies 63 (17), 1–20. https://doi.org/10.1007/s10347-017-0499-7.

Brunović, D., Miko, S., Hasan, O., Papatheodorou, G., Ilijanić, N., Miserocchi, S., Correggiari, A., Geraga, M., 2020. Late Pleistocene and Holocene paleoenvironmental reconstruction of a drowned kars isolation basin (Lošinj Channel, NE Adriatic Sea). Paleogeogr. Palaeoclim. Palaeoecol. 544, 109587. https://doi.org/10.1016/j.palaeo.2020.109587.

Busetti, M., Volpi, V., Barison, E., Giustiniani, M., Marchi, M., Ramella, R., Wardel, l N., Zanolla, N., 2010a. Meso-Cenozoic seismic stratigraphy and the tectonic setting of the Gulf of Trieste (northern Adriatic). GeoActa, Sp. Pub. 3, 1–14.

Busetti, M., Volpi, V., Nicolich, R., Barison, E., Romeo, R., Baradello, L., Brancatelli, G., Giustiniani, M., Marchi, M., Zanolla, C., Wardell, N., Nieto, D., Ramella, R., 2010b. Dinaric tectonic features in the Gulf of Trieste (northern Adriatic Sea). Boll. Geofis. Teor. Appl. 51 (2–3), 117–128.

Camerlenghi, A., Del Ben, A., Hübscher, C., Forlin, E., Geletti, R., Brancatelli, G., Micallef, A., Saule, M., Facchin, L., 2019. Seismic markers of the Messinian salinity crisis in the deep Ionian Basin. Basin Res. 32 (4) https://doi.org/10.1111/bre.12392.

Capella, W., Spakman, W., van Hinsbergen, D.J.J., Chertova, M.V., Krijgsman, W., 2019. Mantle resistance against Gibraltar slab dragging as a key cause of the Messinian Salinity Crisis. Terra. Nova 32, 141–150. https://doi.org/10.1111/ter.12442.

Catuneanu, O., 2006. Principles of Sequence Stratigraphy. Elsevier, Amsterdam, p. 375pp.

Cazzini, F., Zotto, O., Fantoni, R., Ghielmi, M., Ronchi, P., Scotti, P., 2015. Oil and gas in the Adriatic foreland, Italy. J. Petrol. Geol. 38 (3), 255–279. https://doi.org/10.1111/jpg.12610.

Channell, J.E.T., D'Argenio, B., Horváth, F., 1979. Adria, the African promontory, in Mesozoic Mediterranean palaeogeography. Earth Sci. Rev. 15, 213–292.

Civile, D., Lodolo, E., Alp, H., Ben-Avraham, Z., Cova, A., Baradello, L., Accettella, D., Burca, M., Centonze, J., 2014. Seismic stratigraphy and structural setting of the adventure plateau (Sicily Channel). Mar. Geophys. Res. 35, 37–53. https://doi.org/10.1007/s11001-013-9205-5.

Cornée, J.J., Münch, P., Achalhi, M., Merzeraud, G., Azdimousa, A., Quillévéré, F., Melinte-Dobrinescu, M., Chaix, C., Ben Moussa, A., Lofi, J., Séranne, M., Moissette, P., 2016. The Messinian erosional surface and early Pliocene flooding in the Alboran Sea: new insights from Boudinar basin, Morocco. Sediment. Geol. 333, 115–129. https://doi.org/10.1016/j.sedgeo.2015.12.014.

Ćosović, V., Drobne, K., Moro, A., 2004. Paleoenvironmental model for Eocene foraminiferal limestones of the Adriatic carbonate platform (Istrian Peninsula). Facies 50, 61–75.

Del Ben, A., 2002. Interpretation of the CROP M-16 seismic section in the central Adriatic Sea. Mem. Soc. Geol. It. 57, 327–333.

Del Ben, A., Oggioni, F., 2016. Seismic evidence of the rebound of the Adria foreland and the current geodynamics of the Central and Southern Apennines (Italy). J. Geodyn. 99, 51–63. https://doi.org/10.1016/j.jog.2016.06.003.

Del Ben, A., Finetti, I., Rebez, A., Slejko, D., 1991. Seismicity and seismotectonics at the Alps-Dinarides contact. Boll. Geofis. Teor. Appl. 33, 155–176. http://www3.ogs.trieste.it/bgta/provapage.php?id_articolo=328.

Do Couto, D., Popescu, S.M., Pierre Suc, J., Melinte-Dobrinescu, M.C., Barhoun, N., Gorini, C., Jolivet, L., Poort, J., Jouannic, G., Auxietre, J.L., 2014. Lago Mare and the Messinian salinity crisis: evidence from the Alboran sea (S. Spain). Mar. Petrol. Geol. 52, 57–76. https://doi.org/10.1016/j.marpetgeo.2014.01.018.

Fabbri, A., Selli, R., 1972. The structure and stratigraphy of the Tyrrhenian sea. In: Stanley, D.J. (Ed.), The Mediterranean Sea, pp. 75–81.

Fantoni, R., Franciosi, R., 2008. 8 geological sections crossing Po Plain and Adriatic foreland. Rend. online Soc. Geol. It. 3 (2008), 365–366.

Finetti, I.R., Del Ben, A., 2005. Crustal tectono-stratigraphic setting of the Adriatic Sea from new CROP seismic data. In: Finetti, I.R. (Ed.), Deep Seismic Exploration of the Central Mediterranean and Italy, CROP PROJECT. Elsevier, Amsterdam, pp. 519–548.

Fuček, L., Matičec, D., Vlahović, I., Oštrić, N., Prtoljan, B., Korbar, T., Husinec, A., 2012. Basic Geological Map of the Republic of Croatia, Scale 1:50.000, Sheet Cres 2, 1 Sheet. Hrvatski geološki institut, Zavod za geologiju, Zagreb.

Fuček, L., Matičec, D., Vlahović, I., Oštrić, N., Prtoljan, B., Korolija, B., Korbar, T., Husinec, A., Palenik, D., 2015. Basic Geological Map of the Republic of Croatia, Scale 1:50.000, Sheet Cres and Lošinj. Hrvatski geološki institut, Zagreb.

GKRH, 2009. Geological Map of the Republic of Croatia, 1:300.000, 1 Sheet. Hrvatski geološki institut/Croatian Geological Survey, Zagreb. http://webgis.hgi-cgs.hr/gk300/default.aspx.

GKSFRJ, 1970. Geological Map of the SFR Yugoslavia, 1:500.000. 1 sheet Federal geological Institute, Belgrade.

Grandić, S., Biancone, M., Samarzija, J., 2001. Geophysical and stratigraphic evidence of the Triassic rift structuration in the Adriatic offshore area. Nafta 52, 383–396.

Grandić, S., Boromisa-Balaš, E., Šušterčić, M., Kolbah, S., 1999. Hydrocarbon possibilities in the eastern Adriatic slope zone of Croatian offshore area. Nafta 50/2, 51–73.

Grandić, S., Veseli, V., Kolbah, S., 2002. Hydrocarbon potential of Dugi Otok basin in offshore Croatia. Nafta 53, 215–224.

Grandić, S., Kratković, I., Rusan, I., 2010. Hydrocarbon potential assessment of the slope deposits along the SW Dinarides carbonate platform edge. Nafta 61, 325–338.

Grandić, S., Kratković, I., Balić, D., 2013. Peri-Adriatic platforms Proximal Talus reservoir potential (part 1). Nafta 64/2, 147–160.

Hsü, K.J., Montadert, L., Bernoulli, D., Bizon, G., Cita, M., Erickson, A., Wright, R.C., 1978. Site 374: Messinian abyssal plain. In: Initial Reports of the Deep Sea Drilling Project, vol. 42. U.S. Government Printing Office, Washington, DC. Part 1.

Jiménez-Moreno, G., de Leeuw, A., Mandic, O., Harzhauser, M., Pavelić, D., Krijgsman, W., Vranjković, A., 2009. Integrated stratigraphy of the early Miocene lacustrine deposits of pag island (SW Croatia): palaeovegetation and environmental changes in the dinaride lake system. Palaeogeogr. Palaeoclimatol. Palaeoecol. 280, 193–206. https://doi.org/10.1016/j.palaeo.2009.05.018.

Juračić, M., Benac, Č., Crmarić, R., 1999. Seabed and surface sediment map of the Kvarner region, Adriatic Sea, Croatia (lithological map, 1:500,000). Geol. Croat. 52/2, 131–140. https://doi.org/10.4154/GC.1999.11.

Kastelic, V., Carafa, M.M.C., 2012. Fault slip rates for the active External Dinarides thrust-and-fold belt. Tectonics 31, 1–18. https://doi.org/10.1029/2011TC003022.

Korbar, T., 2009. Orogenic evolution of the external Dinarides in the NE adriatic region: a model constrained by tectonostratigraphy of upper cretaceous to Paleogene carbonates. Earth Sci. Rev. 93, 296–312. https://doi.org/10.1016/j.earscirev.2009.07.004.

Korbar, T., Fuček, L., Palenik, D., Matičec, D., Brčić, V., 2010. Overturned Cretaceous to Paleogene carbonates of the NE margin of Vinodol valley – implications for tectonic structure of wider Rijeka region. In: Horvat, M. (Ed.), 4. Croatian Geological Congress with International Participation, pp. 394–395.

Le Breton, E., Handy, M.R., Molli, G., Ustaszewski, K., 2017. Post-20 Ma motion of the Adriatic plate: new constraints from surrounding Orogens and implications for crust-mantle decoupling. Tectonics 36, 3135–3154. https://doi.org/10.1002/2016TC004443.

Lofi, J., 2018. Atlas of the "Messinian Salinity Crisis" Seismic Markers in the Mediterranean Sea-, vol. 2. Co-edition : CCGM & BSGF.

Magaš, N., 1965. Basic Geological Map of SFRY 1:100000, Sheet Cres L-33-113. Institut za geološka istraživanja Zagreb, Federal Geological Institute, Beograd.

Marjanac, T., 1996. Deposition of megabeds (megaturbidites) and sea-level change in a proximal part of the Eocene-Miocene flysch of central Dalmatia (Croatia). Geology 24, 543546. https://doi.org/10.1130/0091-7613(1996)024<0543:DOMMAS>2.3.CO;2.

Marjanac, T., Marjanac, Lj, 2007. Sequence stratigraphy of Eocene incised valley clastics and associated sediments, Island of Rab, northern Adriatic Sea, Croatia. Facies 53, 493–508. https://doi.org/10.1007/s10347-007-0120-6.

Matičec, D., Vlahović, I., Velić, I., Tišljar, J., 1996. Eocene limestones overlying lower cretaceous deposits of western lstria (Croatia): did some parts of present lstria form land during the cretaceous? Geol. Croat. 49/1, 117–127. https://doi.org/10.4154/GC.1994.46.

Mattavelli, L., Novelli, L., Anelli, L., 1991. Occurrence of hydrocarbons in the Adriatic basin. In: Spencer, A.M. (Ed.), Generation, Accumulation, and Production of Europe's Hydrocarbon. Special Publication of the European Association of Petroleum Geoscientists, pp. 369–380.

Müller, R.D., Zahirovic, S., Williams, S.E., Cannon, J., Seton, M., Bower, D.J., et al., 2019. A global plate model including lithospheric deformation along major rifts and orogens since the Triassic. Tectonics 38, 1884–1907. https://doi.org/10.1029/2018TC005462.

Nicolai, C., Gambini, R., 2007. Structural architecture of the Adria-platform-and-basin system. In: Mazzotti, A., Patacca, E., Scandone, P. (Eds.), Results of the CROP Project, Sub-project CROP-04, Southern Apennines (Italy), vol. 7. Boll. Soc. Geol. Ital. Special Issue, pp. 21–37.

Palenik, D., Matičec, D., Fuček, L., Matoš, B., Herak, M., Vlahović, I., 2019. Geological and structural setting of the vinodol valley (NW adriatic, Croatia): insights into its tectonic evolution based on structural investigations. Geol. Croat. 72/3, 179–193. https://doi.org/10.4154/gc.2019.13.

Pamić, J., Gušić, I., Jelaska, V., 1998. Geodynamic evolution of the central Dinarides. Tectonophysics 297, 251–268. https://doi.org/10.1016/S0040-1951(98)00171-1.

Placer, L., Košir, A., Popit, T., Šmuc, A., Juvan, G., 2004. The buzet thrust fault in Istria and overturned carbonate megabeds in the Eocene flysch of the dragonja valley (Slovenia). Geologija 47, 193–198.

Placer, L., Vrabec, M., Celarc, B., 2010. The bases for understanding of the NW Dinarides and Istria Peninsula tectonics. Geologija 53/1, 58–86. https://doi.org/10.5474/geologija.2004.015.

Polšak, A., Šikić, D., 1973. Basic Geological Map of SFRY 1:100000, Sheet Rovinj L 33-100, Explanatory Notes for the Rovinj Sheet. Institut za geološka istraživanja Zagreb, Federal Geological Institute, Beograd, p. 51.

Prelogović, E., Aljinović, B., Bahun, S., 1995. New data on structural relationship in The north dalmatian dinaride area. Geol. Croat. 48/2, 167–176. https://doi.org/10.4154/GC.1995.14.

Prtoljan, B., Jamičić, D., Cvetko Tešović, B., Kratković, I., Markulin, Ž., 2007. The influence of Late Cretaceous synsedimentary deformation on the Cenozoic structuration of the middle Adriatic, Croatia. Geodin. Acta 20/5, 287–300. https://doi.org/10.3166/ga.20.287-300.

Roveri, M., Gennari, R., Grossi, F., Lugli, S., Manzi, V., Iaccarino, S.M., Taviani, M., 2006. The record of Messinian events in the Northern Apennines foredeep basins. Acta Nat. Ateneo Parmense 42/3, 47–123.

Schmid, S.M., Fügenschuh, B., Kounov, A., Matenco, L., Nievergelt, P., Oberhänsli, R., Pleuger, J., Schefer, S., Schuster, R., Tomljenović, B., Ustaszewski, K., van Hinsbergen, D.J.J., 2020. Tectonic units of the Alpine collision zone between Eastern Alps and western Turkey. Gondwana Res. 78, 308–374. https://doi.org/10.1016/j.gr.2019.07.005.

Shaw, J.H., Connors, C., Suppe, J., 2004. Seismic interpretation of contractional fault-related folds. In: An AAPG Seismic Atlas, Studies in Geology, 53, Tulsa, Oklahoma, USA.

Stampfli, G.M., 2005. Plate tectonics of the Apulia-Adria Microcontinents. In: Finetti, I.R. (Ed.), Deep Seismic Exploration of the Central Mediterranean Region and Italy, CROP Project. Elsevier, pp. 747–766.

Šušnjar, M., Bukovac, J., Nikler, L., Crnolatac, I., Milan, A., Šikić, D., Grimani, I., Vulić, Ž., Blašković, I., 1970. Basic Geological Map of SFRY 1:100000, Crikvenica Sheet L 33-102. Institut za geološka istraživanja Zagreb, Federal Geological Institute, Beograd.

Tari, V., 2002. Evolution of the northern and western Dinarides: a tectonostratigraphic approach. EGU Stephan Mueller Spec. Publ. Ser. 1, 223–236. https://doi.org/10.5194/smsps-1-223-2002.

Tari Kovačić, V., Mrinjek, E., 1994. The role of Paleogene clastics in the tectonic interpretation of northern dalmatia (S Croatia). Geol. Croat. 47/1, 127–138. https://doi.org/10.4154/GC.1994.10.

Tomljenović, B., Herak, M., Herak, D., Kralj, D., Kralj, K., Prelogović, E., Bostjančić, I., Matoš, B., 2009. Active tectonics, seismicity and seismogenic sources of the Adriatic coastal and offshore region of Croatia. In: Slejko, D., Rebez, A. (Eds.), 28 Convegno Nazionale "Riassunti Estesi Delle Comunicazioni", pp. 133–136.

Tomljenović, B., Herak, M., Velić, I., Matoš, B., Velić, J., Cota, L., Bejdić, G., Troskot-Čorbić, T., Veseli, V., 2013. Double-Vergent thrusting in the external Dinarides of Croatia: consequences on deposition, tectonics and hydrocarbon system evolution. In: AAPG 2013 European Regional Conference & Exhibition, Barcelona, Spain.

Tomljenović, B., Balling, P., Matoš, B., Vlahović, I., Schmid, S., Ustaszewski, K., Blažok, L., Posarić, D., Širol, A., 2018. Structural architecture and tectonic evolution of the Mt. Velebit in the central part of the External Dinarides in Croatia. In: Neubauer, F., Brendel, U., Friedl, G. (Eds.), International Congress of the Carpathian Balkan Geological Association (CBGA), ABSTRACTS, Advances of Geology in Southwest European Mountain Belts.

Ustaszewski, K., Herak, M., Tomljenović, B., Herak, D., Matej, S., 2014. Neotectonics of the Dinarides–Pannonian Basin transition and possible earthquake sources in the Banja Luka epicentral area. J. Geodyn. 82, 52–68. https://doi.org/10.1016/j.jog.2014.04.006.

van Hinsbergen, D.J.J., Torsvik, T.H., Schmid, S.M., Matenco, L.C., Maffione, M., Vissers, R., Gürer, D., Spakman, W., 2020. Orogenic architecture of the Mediterranean region and kinematic reconstruction of its tectonic evolution since the Triassic. Gondwana Res. 81, 79–229. https://doi.org/10.1016/j.gr.2019.07.009.

van Unen, M., Matenco, L., Nader, F.H., Darnault, R., Mandic, O., Demir, V., 2019. Kinematics of foreland-vergent crustal accretion: inferences from the Dinarides evolution. Tectonics 38, 49–76. https://doi.org/10.1029/2018TC005066.

Vaniček, V., 2013. Pleistocenic Deposits in Croatian Part of Adriatic Subsea. PhD dissertation, vol. 285. University of Zagreb, Faculty of Mining, Geology and Petroleum Engineering.

Velić, J., Malvić, T., 2011. Depositional conditions during Pliocene and Pleistocene in Northern Adriatic and possible lithostratigraphic division of these rocks. Nafta 62, 25–32.

Velić, I., Tišljar, J., Vlahović, I., Matičec, D., Bergant, S., 2003. Evolution of the istrian part of the adriatic carbonate platform from the middle Jurassic to the santonian and formation of the flysch basin during the Eocene: main events and regional comparison. In: Vlahović, I., Tišljar, J. (Eds.), Evolution of Depositional Environments from the Palaeozoic to the Quaternary in the Karst Dinarides and the Pannonian Basin. Field Trip Guidebook 22nd IAS Meeting of Sedimentology, Opatija September 17–19, 2003, Zagreb, pp. 3–17.

Velić, J., Malvić, T., Cvetković, M., Velić, I., 2015. Stratigraphy and petroleum geology of the Croatian part of the adriatic basin. J. Petrol. Geol. 38/3, 281–300. https://doi.org/10.1111/jpg.12611.

Vlahović, I., Tišljar, J., Velić, I., Matičec, D., 2005. Evolution of the adriatic carbonate platform: palaeogeography, main events and depositional dynamics. Palaeogeogr. Palaeoclimatol. Palaeoecol. 220, 333–360. https://doi.org/10.1016/j.palaeo.2005.01.011.

Vlahović, I., Velić, I., Tomljenović, B., Matoš, B., Enos, P., 2018. Massive cenozoic breccia in the Karst Dinarides of Croatia. In: International Congress of the Carpathian Balkan Geological Association (CBGA), ABSTRACTS, Advances of Geology in Southwest European Mountain Belts.

Wacha, L., Mikulčić Pavlaković, S., Frechen, M., Crnjaković, M., 2011. The loess chronology of the island of Susak, Croatia. E G Quat. Sci. J. 60, 153–169. https://doi.org/10.3285/eg.60.1.11.

Wrigley, R., Marszalek, A., Rodriguez, K., Hodgson, N., 2014. Offshore Croatia-hunting 'big oil' in the centre of Europe. First Break 32, 61–68.

Zappaterra, E., 1990. Carbonate paleogeographic sequences of the periadriatic region. Boll. Soc. Geol. Ital. 109, 5–20.

Žibret, L., Vrabec, M., 2016. Palaeostress and kinematic evolution of the orogen-parallel NW-SE striking faults in the NW External Dinarides of Slovenia unraveled by mesoscale fault-slip data analysis. Geol. Croat. 69/3, 295–305. https://doi.org/10.4154/gc.2016.30.